Multicast Scaling of Capacity and Energy Efficiency in Heterogeneous Wireless Sensor Networks

XUECHENG LIU and LUOYI FU, Shanghai Jiao Tong University, China
JILIANG WANG, Tsinghua University, China
XINBING WANG and GUIHAI CHEN, Shanghai Jiao Tong University, China

Motivated by the requirement of heterogeneity in the Internet of Things, we initiate the joint study of capacity and energy efficiency scaling laws in heterogeneous wireless sensor networks, and so on. The whole network is composed of n nodes scattered in a square region with side length $L = n^{\alpha}$, and there are $m = n^{\nu}$ home points $\{c_j\}_{j=1}^{m}$, where a generic home point c_j generates q_j nodes independently according to a stationary and rotationally invariant kernel $k(c_j, \cdot)$. Among the n nodes, we schedule n_s independent multicast sessions each consisting of $k-1$ destination nodes and one source node. According to the heterogeneity of nodes' distribution, we classify the network into two regimes: a cluster-dense regime and a cluster-sparse regime. For the cluster-dense regime, we construct single layer highway system using percolation theory and then build the multicast spanning tree for each multicast session. This scheme yields the $\Omega(n^{\frac{1}{2}+(\alpha-\frac{1}{2})\gamma}/n_s\sqrt{k})$ per-session multicast capacity. For the cluster-sparse regime, we partition the whole network plane into several layers and construct nested highway systems. The similar multicast spanning tree yields the $\Omega(n^{\frac{1}{2}-(1-\nu)\gamma/2}/n_s\sqrt{k})$ per-session multicast capacity, where γ is the power attenuation factor. Interestingly, we find that the bottleneck of multicast capacity attributes to the network region with largest node density, which provides a guideline for the deployment of sensor nodes in large-scale sensor networks. We further analyze the upper bound of multicast capacity and the per-session multicast energy efficiency. Using both synthetic networks and real-world networks (i.e., Greenorbs), we evaluate the asymptotic capacity and energy efficiency and find that the theoretical scaling laws are gracefully supported by the simulation results. To our best knowledge, this is the first work verifying the scaling laws using real-world large-scale sensor network data.

CCS Concepts: • **Networks** → **Packet scheduling**; **Network performance analysis**; *Network experimentation*; • **Computer systems organization** → *Sensor networks*;

Additional Key Words and Phrases: Wireless sensor networks, scaling law, spatial heterogeneity, multicast, capacity, energy efficiency

ACM Reference format:
Xuecheng Liu, Luoyi Fu, Jiliang Wang, Xinbing Wang, and Guihai Chen. 2019. Multicast Scaling of Capacity and Energy Efficiency in Heterogeneous Wireless Sensor Networks. *ACM Trans. Sen. Netw.* 15, 3, Article 33 (May 2019), 32 pages.
https://doi.org/10.1145/3322497

The work is supported by NSFC (61532012, 61822206, 61602303, 61829201), National Key R&D Program of China (2018YFB1004705), CCF Tencent RAGR (20180116), and Agri (X2017010).
Authors' addresses: X. Liu, L. Fu, X. Wang, and G. Chen, Shanghai Jiao Tong University, 800 Dongchuan Rd, Minhang District, Shanghai, China; emails: {liuxuecheng, yiluofu, xwang8}@sjtu.edu.cn, gchen@cs.sjtu.edu.cn; J. Wang, Tsinghua University, Haidian District, Beijing, China; email: jiliangwang@tsinghua.edu.cn.

1550-4859/2019/05-ART33 $15.00
https://doi.org/10.1145/3322497

1 INTRODUCTION

As a novel paradigm, the *Internet of Things* (IoTs) has a wide range of applications [4, 31, 34, 36], including transportation, healthcare, smart environments, and social networks. Among them, a recent trend is to develop highly heterogeneous wireless sensor networks to meet the demands of full interoperation of interconnected devices. While transmitting information collected by sensors [1] requires a high network throughput, off-the-shelf sensor devices suffer from the shortage of electric energy. Meanwhile, throughput and energy efficiency are increasingly becoming vital factors in sensor network designs, since the nowadays broad applications of IoTs require larger size and coverage of sensor networks. To trade off between throughput and energy, multicast, one of the most efficient way of disseminating information so far, serves as the mainstream of all data traffic in wireless sensor networks [18]. In the literature, however, our understanding of both the capacity and energy scaling law of multicast in heterogeneous wireless sensor networks is still limited.

By the virtue of the recent low-cost, low-power implementations of RF radios, hundreds to thousands of these energy-limited sensor nodes are expected to be deployed in the near future. Constrained by the risk of energy shortage, it is necessary to evaluate both the throughput and energy consumption of the network to determine the potential for large-scale deployments that carry delay-tolerant data over energy-limited devices. While capacity in large-scale networks has received much attention over the past two decades [10, 17, 21], the research into the energy efficiency and the relation between energy and capacity remains largely underexplored so far. To gain a fundamental understanding of the intrinsic relation between energy and throughput, in this article we initiate the first study of capacity and energy scaling laws of large -scale heterogeneous networks. Particularly, we suppose that n nodes are randomly scattered on a square region, whose location is modeled by the *cluster process* [5]. Specifically, we first generate m home points $C = \{c_j\}_{j=1}^{m}$ forming a uniform grid, and then each home point c_j generates roughly n/m nodes independently based on a stationary and rotationally invariant kernel $k(c_j, \cdot)$. By assuming n_s independent multicast sessions $\{\mathcal{M}_j\}_{j=1}^{n_s}$ each containing one source node and $k-1$ destination nodes, we are interested in the asymptotic behavior of multicast capacity and energy efficiency as the number of nodes n goes to infinity. Here the multicast capacity refers to the minimum per-session throughput, and multicast energy efficiency is defined as the ratio between minimum capacity and the energy consumed in one multicast session under the capacity achieving scheme.

Different from the spatial uniform distribution, it is more intricate to design the routing and scheduling scheme in spatial heterogeneous network. The main challenge comes from the spatial heterogeneity that results in non-uniform interference and spectrum sharing. Our main idea of taming the difficulty is to look into the cluster-dense and -sparse regime, respectively, where we try to seek for solutions from the most relevant state-of-the-art literature. To elaborate, inspired by the percolation exploited in Reference [10] to derive information capacity, for the cluster-dense regime we build the one layer highway system from a subset of nodes with constant density. For the cluster-sparse regime, it has been shown in Reference [3] that building just one layer highway system is extremely inefficient with respect to the throughput. As an alternative, we build nested highways with different densities to resolve this obstacle. Upon the (nested) highway systems, we construct multicast spanning tree to route the data for each multicast session. We analyze the performance of the percolation-based routing scheme in terms of capacity and energy efficiency and provide an upper bound by means of max-flow and min-cut. We find that the minimum per-flow multicast capacity is constrained by the region with largest node density, which provides a guideline for the deployment of heterogeneous sensor networks. The scaling results are summarized in Tables 1 and 2.

Table 1. The Per-flow Throughput in Different Regimes

	cluster-dense	cluster-sparse
lower bound	$\Omega\left(\frac{n^{\frac{1}{2}+(\alpha-\frac{1}{2})\gamma}}{n_s\sqrt{k}}\right)$	$\Omega\left(\frac{n^{\frac{1}{2}-(1-\nu)\gamma/2}}{n_s\sqrt{k}}\right)$
upper bound	$O\left(\frac{L^\gamma(qs(d_c))^{\gamma/2}}{n_s\sqrt{k}}\right)$	$O\left(\frac{L^\gamma(qs(d_c))^{\gamma/2}}{n_s\sqrt{k}}\right)$

Table 2. The Energy Efficiency in Different Regimes

	cluster-dense	cluster-sparse
lower bound	$\Omega\left(\frac{n^{\frac{1}{2}+(\alpha-\frac{1}{2})\gamma}}{n_s k(\sqrt{k}+\sqrt{n})}\right)$	$\Omega\left(\frac{n^{\frac{1}{2}-(1-\nu)\gamma/2}}{n_s k(\sqrt{k}+\sqrt{n})}\right)$
upper bound	$O\left(\frac{L^\gamma(qs(d_c))^{\gamma/2}}{n_s k(\sqrt{k}+\sqrt{n})}\right)$	$O\left(\frac{L^\gamma(qs(d_c))^{\gamma/2}}{n_s k(\sqrt{k}+\sqrt{n})}\right)$

Main contributions of this work:

- To the best of our knowledge, this is the first work to study both the capacity and energy efficiency scaling law of multicast in spatially heterogeneous network. We leverage the *cluster process* [5] to model the heterogeneous distribution of sensor nodes in practical IoT architecture.
- Based on the heterogeneity of nodes' distribution, we classify the network into two regimes: a *cluster-dense* regime and a *cluster-sparse* regime. Inspired from percolation theory, we construct (nested) highways and build multicast spanning tree to find the scaling law lower bound. Interestingly, we find that the minimum per-session multicast capacity is constrained by the region covered with densest nodes.
- We evaluate the performance of proposed routing and scheduling schemes on both synthetic networks and real-world networks (i.e., the international large-scale sensor network system GreenOrbs [26]). We find that the scaling law achieved by the schemes is well approximated by the analytical results.

The rest of this article is organized as follows: Section 2 gives a brief overview of the state of the art. In Section 3, the system models are presented and asymptotic capacity and energy efficiency are defined. Several technical lemmas are described in Section 4. Sections 5 and 6 analyze the cluster-dense and cluster-sparse regimes, respectively. The capacity upper bound is discussed in Section 7, and the energy efficiency is investigated in Section 8. Simulations regarding capacity and energy efficiency are outlined in Section 9. The conclusions are drawn in Section 10.

2 RELATED WORK

There is a vast amount of literature on scaling laws in large-scale wireless (sensor) networks, which can be classified according to the traffic patterns and spatial distribution of nodes:

- Unicast for uniformly distributed nodes: Unicast refers to the traffic pattern in which one source node transmits data to one destination node. Gupta and Kumar showed in their seminar paper [17] that the capacity is upper bounded by $O(\frac{1}{\sqrt{n}})$ and lower bounded by $\Omega(\frac{1}{\sqrt{n\log n}})$. Franceschetti et al. later proved that $\Theta(\frac{1}{\sqrt{n}})$ capacity is achievable by a percolation based routing and scheduling scheme [10].

- Multicast for uniformly distributed nodes: Multicast refers to the traffic pattern in which one source node transmits data to multiple destination nodes. It is typically assumed that there are n_s multicast sessions and each session contains n_d nodes. Shakkottai et al. showed in Reference [30] that the per-session multicast capacity is upper bounded by $O(\frac{\sqrt{n}}{n_s\sqrt{n_d \log n}})$, and when $n_s\sqrt{n_d} = \Omega(\sqrt{n \log n})$ the $\Theta(\frac{\sqrt{n}}{n_s\sqrt{n_d \log n}})$ capacity is achievable using a comb-based architecture. Li proved [23] that when $n_d = O(\frac{n}{\log n})$ the multicast capacity is $\Theta(\frac{\sqrt{n}}{n_s\sqrt{n_d \log n}})$, and when $n_d = \Omega(\frac{n}{\log n})$ the multicast capacity is $\Theta(\frac{1}{n_s})$. Later, Li et al. considered a different channel model called the *Gaussian channel model* and showed that the multicast capacity is upper bounded by $O(\frac{\sqrt{n}}{n_s\sqrt{n_d}})$ when $n_d = O(\frac{n}{\log^2 n})$ and $n_s = \Omega(\log n)$, and the multicast capacity is lower bounded by $\Omega(\frac{\sqrt{n}}{n_s\sqrt{n_d}})$ under some constraints on n_d and n_s [24].
- Data collection for uniformly distributed nodes: Data collection refers to the traffic pattern in which multiple source nodes transmit data to one common destination node. E. J. Duarte-Melo and M. Liu showed that the per-session capacity is $\Theta(\frac{1}{n})$ in Reference [9] and analyzed the energy efficiency in Reference [8].
- Unicast for clustered distributed nodes: Alfano et al. studied both the upper and lower bounds of per-session unicast capacity assuming that the nodes are distributed according to the shot-noise Cox processes [2, 3].

To the best of our knowledge, there is very little work that attempts to explore the capacity scaling laws for multicast traffic pattern and clustered distribution of nodes. Most closely related to our work is the contribution [25] by Li et al., who studied the multicast capacity under interference protocol model for static ad hoc networks with heterogeneous clusters. They assumed that the cluster head is the source node and all the other nodes in that cluster are the sink nodes. In contrast to their paper, we considered the Gaussian channel model and the multicast traffic pattern in which the source node do not need to be the cluster head and the destination nodes could be distributed in different clusters.

Another issue of great interest is energy consumption in wireless (sensor) networks. Gamal et al. [12] addressed the minimum energy per bit requirement for reliable communication via a general class of channels. Later, Jain et al. extended the results to broadcast in static wireless networks [19, 20]. Recently, there has been growing interest in developing energy efficient protocols and algorithms for networking and computer systems. In Reference [35], Wieselthier et al. constructed energy efficient broadcast and multicast trees in wireless networks. Fu et al. [11] proposed a new framework called ConMap that jointly optimizes both the transmitting and receiving energy in delay constrained mobile wireless networks. Mobility of sensor nodes are exploited to improve the energy efficiency in data collection networks [6, 13, 27, 28, 37].

3 SYSTEM MODEL

In this section, we present the network model, channel model, traffic model, and definitions of asymptotic capacity and energy efficiency. We summarize the frequently used notations in Table 3.

3.1 Heterogeneous Network Model

We consider extended networks composed of n i.i.d. nodes over a square region $\mathcal{B}$ of side length $L = n^\alpha$, with $\alpha \geq 0$. To avoid border effects, we consider wraparound conditions at the network edges (i.e., the network area is assumed to be the surface of a bidimensional torus).

Table 3. Notations Used in This Article

Notation	Definition
$\mathcal{B}$	square region of heterogeneous network
$\mathbf{C}$	positions of cluster centers
$k(c_j, \cdot)$	kernel function of cluster process
$\Phi(\xi)$	local intensity at point ξ
$\mathbf{V}$	collection of nodes' positions in a given realization of the cluster process
$s(\rho)$	nonnegative, nonincreasing continuous function used to define kernel
d_c	distance between two neighboring cluster centers on the grid
$l_{ij}(d_{ij})$	power attenuation between i and j
n_s	number of multicast sessions in the network
n	number of nodes in the network
k	number of nodes in each multicast session
$\lambda^{\min}(n)$	minimum per-flow multicast throughput
$\mathcal{E}_{\mathcal{S}}$	energy vector of the n_s multicast flows
$\eta(n)$	per-flow energy efficiency
EST($\mathcal{M}$)	Euclidean spanning tree for multicast session $\mathcal{M}$
EMST($\mathcal{M}$)	Euclidean minimum spanning tree for multicast session $\mathcal{M}$
MT($\mathcal{M}$)	multicast tree for multicast session $\mathcal{M}$
$\{\mathcal{B}_h\}$	nested domains in the cluster-sparse regime
$\{\Delta\mathcal{B}_h\}$	a partition of network $\mathcal{B}$ in the cluster-sparse regime
$\mathcal{H}$	highway system

To characterize the heterogeneity of nodes' spatial distribution, we assume that nodes are deployed according to a *cluster process* [5] defined as follows:

(1) First, specify a point process $C = \{c_j\}_{j=1}^{m}$ of cluster centers, where $m = n^{\nu}$ and $\nu \in (0, 1)$. In the literature, the cluster center c_j is also called parent or home point.
(2) Second, each home point c_j independently generates point processes of nodes whose intensity at $\xi \in \mathcal{B}$ is given by $q_j k(c_j, \xi)$, where $k(c_j, \cdot)$ is a kernel function and $q_j > 0$ is the number of nodes generated by home point c_j.
(3) Third, the overall node process is given by the superposition of the independent individual processes generated by the home points. According to Campbell's formula [5], the local intensity at $\xi \in \mathcal{B}$ of the cluster process is

$$\Phi(\xi) = \sum_{j=1}^{m} q_j k(c_j, \xi).$$

We remark that this assumption is prevalent in the study of spatial heterogeneity in wireless networks [2, 3, 25]; therefore we do not focus on the formation of clustering. To simplify the analysis, we assume that m home points are deterministically deployed over the vertices of a square grid, i.e., the point process C is a uniform grid. Let d_c denote the distance between two neighboring home point on the grid, then

$$d_c = L/\sqrt{m} = n^{\alpha - \nu/2}. \tag{1}$$

We shall classify the network into two regimes according to the asymptotic behavior of d_c:

- *cluster-dense* regime: $\lim_{n\to\infty} d_c = 0$, *i.e.*, $\alpha < \nu/2$;
- *cluster-sparse* regime: $\lim_{n\to\infty} d_c = \infty$, *i.e.*, $\alpha > \nu/2$.

It should be noted that this simplification does not alter the scaling laws achieved by other slightly more complicated uniform point processes. Furthermore, we assume that each home point generates the same number of nodes, i.e., $q_j = q = n^{1-\nu}$ for all $j = 1, \ldots, m$, despite that this restriction could be relaxed.

There are many forms of kernel function, among which the stationary and rotationally invariant kernel is widely used to model the clustering and heterogeneity of networks [2, 3, 14, 15]. For the tractability, we assume that $k(c_j, \xi) = k(|\xi - c_j|)$ is a nonnegative, nonincreasing, bounded, and continuous function with integral $\int_{\mathcal{B}} k(c_j, \xi) d\xi = 1$, where $|\xi - c_j|$ denotes the Euclidean distance between c_j and ξ. Moreover, we assume

$$k(c_j, \xi) = \frac{s(|\xi - c_j|)}{\int_{\mathcal{B}} s(|\zeta - c_j|) d\zeta},$$

where $s(\rho)$ is a nonnegative, nonincreasing continuous function satisfying $\int_0^\infty \rho s(\rho) d\rho < \infty$. Notice that $k(c_j, \xi) = \Theta(s(|\xi - c_j|))$ if we neglect the normalizing factor $\int_{\mathcal{B}} s(|\zeta - c_j|) d\zeta = \Theta(1)$. For concreteness, we take $s(\rho)$ as $s(\rho) = \min(1, \rho^{-\delta})$ whose tail decays as a power law for $\delta > 2$, though our results apply to more general shapes as well.

For convenience, we use $\mathbf{V} = \{v_i\}_{i=1}^n$ to denote the set of nodes as well as locations.

3.2 Gaussian Channel Model

Time is divided into slots of equal duration, and in each slot a set of transmitters are enabled to communicate with corresponding receivers over Gaussian channels of unit bandwidth. We assume point-to-point coding and decoding, and hence signals received from nodes other than the (unique) transmitter are regarded as noise. Considering the limited battery of sensor devices, we assume that the power emitted by each node ranges from $\underline{P}$ to $\overline{P}$, where $0 < \underline{P} \leq \overline{P} < \infty$.

In this *Gaussian channel model* [3, 10, 17, 24], the data rate achievable by node v_i transmitting to node v_j in a given time slot is

$$R_{ij} = \log(1 + \mathrm{SINR}_{ij}), \tag{2}$$

where SINR_{ij} is the signal-to-interference-plus-noise ratio at receiver v_j:

$$\mathrm{SINR}_{ij} = \frac{P_i l_{ij}}{N_0 + \sum_{k \in \mathcal{T}, k \neq i} P_k l_{kj}}. \tag{3}$$

Here $\mathcal{T}$ is the set of nodes that are enabled to transmit in the given slot, P_i is the power emitted by node i, l_{ij} is the power attenuation between i and j, and N_0 is the ambient noise power. To account for near-field propagation effect, the power attenuation is assumed to be a deterministic function of the distance d_{ij} between i and j, according to $l_{ij}(d_{ij}) = \min\{1, d_{ij}^{-\gamma}\}$, with $\gamma \geq 2$.

3.3 Multicast Traffic Model

Assume that there are n_s random multicast sessions each with size k. The process of generating these multicast sessions are as follows. Randomly pick n_s nodes from all the n nodes to be the sources of the multicast sessions and denote them as $\mathcal{S}$. For each source node, choose $k - 1$ nodes as its intended receivers without replacement. In total we will have n_s multicast sessions $\{\mathcal{M}_i\}_{i=1}^{n_s}$ where $\mathcal{M}_i$ is a multicast session. Note that sometimes $\mathcal{M}_i \cap \mathcal{M}_j \neq \varnothing$ for any $i \neq j$.

When $n_s = n$ and $k = 2$, the traffic reduces to *unicast* with $\Theta(n)$ sources; to make a difference, we assume that $\lim_{n \to \infty} n_s = \infty$ and $\lim_{n \to \infty} k = \infty$.

3.4 Asymptotic Capacity and Energy Efficiency

For any static network $G = (V, E)$, the node positions $\mathbf{V}$, the set $\mathcal{S}$ of n_s source nodes, and the set of receivers for each source node are all fixed. Let $\lambda_{\mathcal{S}} = (\lambda_1, \ldots, \lambda_{n_s})$ be the rate vector of the n_s

source nodes, where λ_i is the data rate of source node s_i. We say that a multicast rate vector $\lambda_{\mathcal{S}}$ bits/s is *feasible* if there exists a spatial and temporal scheme such that by operating the network in a multihop and store-and-forward manner, every source node s_i can send λ_i bits/s on average to its $k-1$ destination nodes. That is, there exists a finite constant $T < \infty$ such that in every time interval of duration T, every source node $s_i \in \mathcal{S}$ can send $T \cdot \lambda_i$ bits to its corresponding $k-1$ receivers *w.h.p.*

From the rate vector $\lambda_{\mathcal{S}}$, we could define the aggregated throughput as $\Lambda_{\mathcal{S}}(n) = \sum_{i=1}^{n_s} \lambda_i$, the average throughput as $\lambda_{\mathcal{S}}^{\text{avg}}(n) = \sum_{i=1}^{n_s} \lambda_i / n_s$, the minimum throughput as $\lambda_{\mathcal{S}}^{\min}(n) = \min_i\{\lambda_i\}$. The metric comes into our interest is the minimum throughput $\lambda^{\min}(n)$, which we refer to as *per-session multicast capacity* and $\mathcal{S}$ is dropped from the notations if it is clear. We give the formal definition of asymptotic capacity as follows.

Definition 3.1 (Asymptotic Per-session Multicast Capacity). We say that the *per-session multicast capacity* of a class of random networks is of order $\Theta(f(n))$ bits/s if there exists constants c, c' such that $0 < c < c' < +\infty$ and

$$\lim_{n\to\infty} \Pr(\lambda^{\min}(n) = cf(n) \text{ is feasible}) = 1$$
$$\liminf_{n\to\infty} \Pr(\lambda^{\min}(n) = c'f(n) \text{ is feasible}) < 1.$$

Since the achievable throughput is constrained by energy through Equation (2) and Equation (3), it is necessary to quantify the energy required by the achievable throughput and corresponding energy efficiency. Previous work [29, 33] has suggested the concept of bits-per-joule capacity to evaluate how much information can be transmitted with each unit energy. Along with the feasible rate vector $\lambda_{\mathcal{S}}$, let $\mathcal{E}_{\mathcal{S}} = (E_1, \ldots, E_{n_s})$ be the energy vector of the n_s multicast flows, where E_i is the energy consumed by the nodes serving the multicast flow of source node i. Define the average energy as $E_{\mathcal{S}}^{\text{avg}} = \sum_{i=1}^{n_s} E_i / n_s$. We refine the definition of energy efficiency in Ref. [29] and define the energy efficiency $\eta(n)$ as the ratio of the minimum throughput $\lambda^{\min}(n)$ and the required minimum average energy $E^{\text{avg}}(n)$. The asymptotic energy efficiency is given as follows.

Definition 3.2 (Asymptotic Per-session Energy Efficiency). We say that the *per-session energy efficiency* $\eta(n)$ is of order $\Theta(g(n))$ bits/s/Joule if there exists constants c, c' such that $0 < c < c' < +\infty$ and

$$\lim_{n\to\infty} \Pr(\eta(n) = cg(n) \text{ is feasible}) = 1$$
$$\liminf_{n\to\infty} \Pr(\eta(n) = c'g(n) \text{ is feasible}) < 1.$$

4 PRELIMINARIES

In this section, we present some lemmas that will be used in later analysis. The first is the achievable data rate per link restricted by some physical constraints.

Lemma 4.1 (Achievable Data Rate) [22]. *At any time, assume that for any sender–receiver pair (s_i, v_i) the following conditions hold:*

- *C1: The Euclidean distance $|s_i - v_i| \leq r$;*
- *C2: For any other sender $s_k, k \neq i$, the Euclidean distance $|s_k - v_i| \geq R > r$;*
- *C3: The power emitted by each sender is P.*

Then, each receiver can receive at rate at least

$$\log\left(1 + \frac{P \cdot l(r)}{N_0 + c_1 P (R-r)^{-\gamma}}\right),$$

where c_1 is a constant only depending on γ.

The second is the node density of point processes.

Lemma 4.2. *Consider a set* $\mathbf{U}$ *of points distributed over the network region* $\mathcal{B}$ *according to a homogeneous Poisson point process (HPP) of rate* Φ*. Let* $\mathcal{A} = \{A_k\}$ *be a regular tessellation of* $\mathcal{B}$ *(or any subregion of* $\mathcal{B}$*) whose tiles* A_k *have a surface* $|A_k|$ *non smaller than* $24\frac{\log n}{\Phi}$*. Let* $N(A_k)$ *be the number of points of* $\mathbf{U}$ *falling in* A_k*. Then uniformly over the tessellation,* $N(A_k)$ *is* w.h.p. *between* $\frac{\Phi|A_k|}{2}$ *and* $2\Phi|A_k|$*, i.e.,* $\frac{\Phi|A_k|}{2} < N(A_k) < 2\Phi|A_k|$.

Lemma 4.3 (Asymptotic Local Intensity). *In a cluster-dense regime,* $\Phi(\xi) = \Theta(n/L^2)$ *for all* $\xi \in \mathcal{B}$*; in a cluster-sparse regime,* $\Phi(\xi) = \Theta(qs(\min_j |\xi_0 - c_j|))$ *for all* $\xi \in \mathcal{B}$.

Denote the bounds of intensity as $\overline{\Phi} = \sup_{\xi\in\mathcal{B}} \Phi(\xi)$ and $\underline{\Phi} = \inf_{\xi\in\mathcal{B}} \Phi(\xi)$. From Lemma 4.3, we have the following corollary.

Corollary 4.4. *In a cluster-dense regime,* $\underline{\Phi} = \Theta(\overline{\Phi}) = \Theta(n/L^2)$*; in a cluster-sparse regime,* $\underline{\Phi} = \Theta(qs(d_c))$ *and* $\overline{\Phi} = \Theta(q)$.

Lemma 4.5 (Thinning IPP) [3]. *Consider a set* $\mathbf{V}$ *of points distributed over a compact region* $\mathcal{B}$ *according to an inhomogeneous Poisson point process (IPP) of intensity* $\Phi(\xi)$*. For any* $\Phi_0 \leq \underline{\Phi}$*, it is possible to extract from* $\mathbf{V}$ *a subset of points* $\mathbf{U} \subseteq \mathbf{V}$ *distributed over* $\mathcal{B}$ *according to a HPP of rate* Φ_0.

The third is the percolation and connectivity. Consider the independent bond percolation model on the square lattice. That is, we declare each edge of an infinite square grid *open* with probability p and *closed* otherwise, independently of all other edges. Let B_m denote a box of side length m embedded in the square lattice.

For any given $\kappa > 0$, let us partition B_m into rectangles R_m^i of sides $m \times (\kappa \log m - \epsilon_m)$. We choose $\epsilon_m > 0$ as the smallest value such that the number of rectangles $\frac{m}{\kappa \log m - \epsilon_m}$ in the partition is an integer. It is easy to see that $\epsilon_m = o(1)$ as $m \to \infty$. We let C_m^i be the maximal number of edge-disjoint left to right crossings of rectangle R_m^i and let $N_m = \min_i C_m^i$. The result is the following.

Lemma 4.6 [10]. *For all* $\kappa > 0$ *and* $\frac{5}{6} < p < 1$ *satisfying* $2 + \kappa \log(6(1-p)) < 0$*, there exists a* $\delta(\kappa, p) > 0$ *such that*

$$\lim_{m\to\infty} \Pr(N_m \leq \delta \log m) = 0.$$

The fourth is the multicast tree. In the literature, a multicast tree is designed to route multicast packets efficiently. Inspired from Prim's algorithm, the following algorithm build a Euclidean spanning tree using pigeonhole principle.

ALGORITHM 1: Build a Euclidean Spanning Tree EST($\mathcal{M}$)

Input: A multicast session $\mathcal{M}$ consisted of k nodes.
EST($\mathcal{M}$) $\leftarrow \mathcal{M}$;
for $g \leftarrow k-1, k-2, \ldots, 1$ **do**
    Partition the square $\mathcal{B}$ into a $\lfloor\sqrt{g}\rfloor$ by $\lfloor\sqrt{g}\rfloor$ grid with side length $L/\lfloor\sqrt{g}\rfloor$;
    Find a squarelet that contains at least two nodes u and v from different connected components in EST($\mathcal{M}$);
    EST($\mathcal{M}$) $\leftarrow$ EST($\mathcal{M}$) $\cup\, \overline{uv}$;
end
Output: A Euclidean multicast spanning tree EST($\mathcal{M}$).

Lemma 4.7. *The total length of EST($\mathcal{M}$) built by Algorithm 1 is at most* $4\sqrt{2}\sqrt{k}L$.

Proof. EST($\mathcal{M}$) contains $k-1$ edges added by Line 3 to Line 5 in Algorithm 1 for $g = k-1, k-2, \ldots, 1$. For a given g, the edge $\overline{uv}$ is contained in a box with side length $L/\lfloor\sqrt{g}\rfloor$. Notice that $|u-v|$ is no longer than the diagonal length of the box. Thus, the total length of EST($\mathcal{M}$) can be bounded above as follows:

$$|\mathrm{EST}(\mathcal{M})| \leq \sqrt{2}\sum_{g=1}^{k-1}\frac{L}{\lfloor\sqrt{g}\rfloor} \overset{(a)}{\leq} 2\sqrt{2}L\sum_{g=1}^{k-1}\frac{1}{\sqrt{g}} \leq 2\sqrt{2}L\left(1+\int_1^{k-1}\frac{1}{\sqrt{u}}du\right) = 2\sqrt{2}L\left(2\sqrt{k-1}-1\right),$$

where (a) comes from $\lfloor\sqrt{g}\rfloor \geq \sqrt{g}/2$ for $g = 1, 2, \ldots, k-1$. □

The standard work of Steele [32] provides a lower bound for the total length of any Euclidean spanning tree.

Lemma 4.8 [32]. *Suppose that a set $\mathcal{M}$ of k nodes are independently, identically distributed in a bounded subset $\mathcal{B}(\mathbb{R}^d)$ of $\mathbb{R}^d$ with bounded density function $f : \mathbb{R}^d \mapsto [0, +\infty)$. Denote the Euclidean minimum spanning tree of $\mathcal{M}$ as EMST($\mathcal{M}$). As $k \to \infty$, the asymptotic total length of EMST($\mathcal{M}$) is*

$$|EMST(\mathcal{M})| = c(d)k^{\frac{d-1}{d}}\int_{\mathbb{R}^d} f(x)^{\frac{d-1}{d}}dx, \tag{4}$$

where $c(d)$ is a constant depending only on the dimension d.

Corollary 4.9. *If the set $\mathcal{M}$ of k nodes are uniformly at random distributed in a bounded connected domain $\mathcal{S} \subset \mathbb{R}^2$, then as $k \to \infty$, the asymptotic total length of EMST($\mathcal{M}$) is*

$$|EMST(\mathcal{M})| = c(2)\sqrt{k}\sqrt{|\mathcal{S}|},$$

where $|\mathcal{S}|$ denotes the area of domain $\mathcal{S}$.

Lemma 4.10 [7]. *Given any k nodes $\mathcal{M}$, any multicast tree spanning these k nodes (may be using some additional relay nodes) will have an Euclidean length at least $\frac{\sqrt{3}}{2}|EMST(\mathcal{M})|$.*

Lemma 4.11. *For both the cluster-dense and cluster-sparse regimes, the total length of Euclidean minimum spanning tree EMST($\mathcal{M}$) is $|EMST(\mathcal{M})| = \Theta(\sqrt{k}L)$.*

Proof. We scale the region $\mathcal{B}$ of size $L \times L$ to $\mathcal{B}'$ of size 1×1. Recall that for any point $\xi \in \mathcal{B}$, its local density is $\phi(\xi) = \Phi(\xi)/n$. After scaling, the point ξ in $\mathcal{B}$ is mapped into a point ξ' in $\mathcal{B}'$. And the local density at ξ' is $\phi'(\xi') = L^2\phi(\xi)$.

For the cluster-dense regime, $\phi'(\xi') = \Theta(1)$, since $\Phi(\xi) = \Theta(n/L^2)$. According to Lemma 4.8,

$$|\mathrm{EMST}(\mathcal{M}')| = c(2)\sqrt{k}\int_{\mathcal{B}'}\phi'(\xi')d\xi' = \Theta(\sqrt{k}),$$

where $\mathcal{M}'$ is the mapping of $\mathcal{M}$ after scaling. Therefore, we have $|\mathrm{EMST}(\mathcal{M})| = \Theta(\sqrt{k}L)$.

For the cluster-sparse regime, the intensity $\Phi(\xi) = \Theta(qs(d(\xi)))$, where $d(\xi) = \min_{1\leq j\leq m}|\xi - c_j|$. And $\phi'(\xi') = \Theta(d_c^2 s(Ld(\xi')))$, where $d(\xi') = \min_{1\leq j\leq m}|\xi' - c_j'|$. Since $\phi'(\xi')$ is not bounded as $n \to \infty$, the results in Lemma 4.8 cannot be applied directly. Instead, we could approximate the HPP with density function $\phi'(\xi')$ using uniform distribution. Suppose that $k = o(m)$. Notice that nodes in the circle centered at c_j' with radius equal to $1/L$ are distributed uniformly at random with density d_c^2. We can partition the network region $\mathcal{B}'$ into two parts: (1) $\mathcal{B}_1'$ covers all the m circles defined above and (2) $\mathcal{B}_2'$ covers the remaining connected part. For a multicast set $\mathcal{M}$ consisted of k nodes, about

c_1k nodes are distributed in $\mathcal{B}_1'$ and the remaining $(1-c_1)k$ nodes are distributed in $\mathcal{B}_2'$. The total length of multicast tree connecting the nodes in $\mathcal{B}_1'$ is approximately

$$|\mathrm{EMST}(\mathcal{M}' \cap \mathcal{B}_1')| = m \cdot \sqrt{c_1 k/m}/L = \sqrt{c_1 km}/L.$$

If we approximate the heterogeneous node distribution in $\mathcal{B}_2'$ as uniform distribution, then the total length of multicast tree connecting the nodes in $\mathcal{B}_2'$ is approximately

$$|\mathrm{EMST}(\mathcal{M}' \cap \mathcal{B}_2')| = \sqrt{(1-c_1)k}\sqrt{1-m/L^2},$$

and then we have

$$|\mathrm{EMST}(\mathcal{M}')| = |\mathrm{EMST}(\mathcal{M} \cap \mathcal{B}_1')| + |\mathrm{EMST}(\mathcal{M} \cap \mathcal{B}_2')| \sim \sqrt{1-c_1}\sqrt{k}.$$

Suppose that k is $\Theta(m)$ or $O(m)$; then the k nodes are uniformly attached to the cluster centers. We have $|\mathrm{EMST}(\mathcal{M}')| = \sqrt{k}$. □

5 CLUSTER-DENSE REGIME

In this section, we consider the cluster-dense regime in which $\lim_{n\to\infty} d_c = 0$. We propose a percolation-based routing scheme and analyze its performance under the TDMA scheduling scheme.

5.1 Overview of the Scheme

Our routing scheme is built upon the highway system that was first proposed in Reference [10]. The highway system could be easily constructed using percolation theory under the assumption that the nodes are uniformly at random distributed over a square region. However, the density function $\Phi(\xi)$ is not a constant in cluster-dense regime, before applying the percolation theory we shall extract a subset of nodes with constant intensity. Gauranteed by Lemma 4.5, we can first extract a subset of nodes $\mathbf{U}$ with intensity $\underline{\Phi}$ from $\mathbf{V}$. Then we can construct the highway system $\mathcal{H}$ upon the nodes $\mathbf{U}$. Finally, we transform the Euclidean spanning tree $\mathrm{EST}(\mathcal{M})$ obtained from Algorithm 1 to a new multicast tree $\mathrm{MT}(\mathcal{M})$ using the nodes in $\mathcal{H}$. The data are routed through $\mathrm{MT}(\mathcal{M})$, and the time division multiple access method in Reference [21] is used to control the interference.

5.2 Constructing the Highway

The extracted nodes $\mathbf{U}$ forms a HPP with intensity $\underline{\Phi}$ in the whole network region $\mathcal{B}$. To begin the construction of the highway, we partition region $\mathcal{B}$ into small squarelets s_i of side length c, as depicted in Figure 1. Let $N(s_i)$ be the number of nodes from $\mathbf{U}$ inside s_i. By appropriately choosing c, we can arrange that the probability that a square contains at least one node from $\mathbf{U}$ is as high as we want. Indeed, for all i, we have $p \triangleq \Pr(N(s_i) \geq 1) = 1 - e^{-\underline{\Phi}c^2}$. We say that a squarelet is *open* if it contains at least one node and *closed* otherwise.

Notice that squarelets are open (or closed) with probability p (or $1-p$), independently of each other. Hence, we could map this model into a *discrete bond-percolation model* on the square grid: We draw an horizontal edge across half of the squares and a vertical edge across the others, as shown in Figure 1. In this way, we obtain a grid of horizontal and vertical edges, each edge being open, independently of all other edges, with probability p. A path is said to be *open* if it contains only open edges. Denote the number of edges composing the side length of $\mathcal{B}$ by $l = \frac{L}{c\sqrt{2}}$, where c is rounded up such that l is an integer. By Lemma 4.6, we can choose c large enough such that $\frac{5}{6} < p < 1$ and $2 + \kappa \log(6(1-p)) < 0$. Partition the square network region $\mathcal{B}$ into parallel rectangles with size $l \times (\kappa \log l - \epsilon_l)$. Within each rectangle, we can find the highway (a path from left side of the rectangle to the right side of the rectangle) using breadth-first search. In this way, according

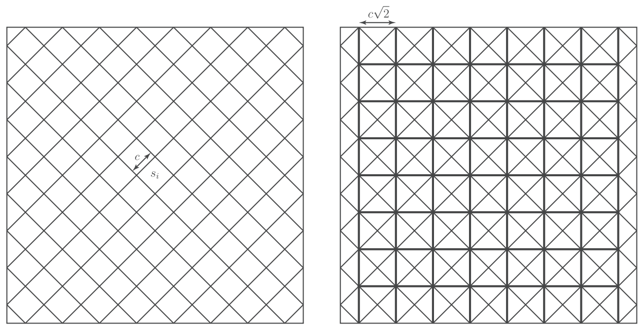

Fig. 1. Construction of the bond percolation model.

to Lemma 4.6, it is guaranteed that there are *w.h.p.* $\Omega(l)$ paths crossing $\mathcal{B}$ from left to right, and these can be grouped into disjoint sets of $\lceil \delta \log l \rceil$ paths, each group crossing a rectangle of size $l \times (\kappa \log l - \epsilon_l)$, for all $\kappa > 0$, δ small enough, and a vanishingly small ϵ_l so that the side length of each rectangle is an integer. The same is true if we divide the area into vertical rectangles and look for paths crossing the area from bottom to top. According to Lemma 4.6, when $c = \Theta(1/\sqrt{\Phi})$ (e.g., $c = \sqrt{\log_e 12}/\sqrt{\Phi}$) there exist both horizontal and vertical disjoint paths *w.h.p.* These paths form a backbone called the *highway*.

After we construct the highway system, we use Algorithm 2 to build a multicast tree for routing. Notice that the multicast trees are independent of each other for different multicast sessions. And if nodes u_1, u_2 are in the same crossing path, then $\mathcal{P}(\overline{u_1u_2})$ represents the path formed by all the nodes from u_1 to u_2 in that crossing path, as shown in Figure 2.

ALGORITHM 2: Build Multicast Tree for Cluster-Dense Regime

Input: A multicast session $\mathcal{M}$ consisted of k nodes.
$\mathrm{MT}'(\mathcal{M}) \leftarrow \mathcal{M}$;
Build a Euclidean multicast spanning tree $\mathrm{EST}(\mathcal{M})$ using Algorithm 1;
for *each edge* $\overline{v_iv_j}$ *in* $EST(\mathcal{M})$ **do**
    Find the corresponding horizontal highway entry point u_i, u_j and vertical highway entry point u'_i, u'_j;
    if u_i *and* u_j *are in the same crossing path* **then**
        $\mathrm{MT}'(\mathcal{M}) \leftarrow \mathrm{MT}'(\mathcal{M}) \cup \overline{v_iu_i} \cup \mathcal{P}(\overline{u_iu_j}) \cup \overline{u_jv_j}$;
    else if u'_i *and* u'_j *are in the same crossing path* **then**
        $\mathrm{MT}'(\mathcal{M}) \leftarrow \mathrm{MT}'(\mathcal{M}) \cup \overline{v_iu'_i} \cup \mathcal{P}(\overline{u'_iu'_j}) \cup \overline{u'_jv_j}$;
    else
        Find a node w_i from the vertical crossing path of node u'_i and a node w_j from the horizontal crossing path of node u_j such that $|w_i - w_j| \leq \sqrt{5}c$;
        $\mathrm{MT}'(\mathcal{M}) \leftarrow \mathrm{MT}'(\mathcal{M}) \cup \overline{v_iu'_i} \cup \mathcal{P}(\overline{u'_iw_i}) \cup \overline{w_iw_j} \cup \mathcal{P}(\overline{w_ju_j}) \cup \overline{u_jv_j}$;
    end
end
$\mathrm{MT}(\mathcal{M}) \leftarrow \mathrm{MT}'(\mathcal{M})$ with redundant edges and loops removed;
Output: A multicast tree $\mathrm{MT}(\mathcal{M})$ using highway system.

5.3 Capacity Analysis

Routed by the multicast tree $\mathrm{MT}(\mathcal{M})$ built from the highway, the single hop transmission could be classified into three cases based on whether the sender and receiver are in the highway:

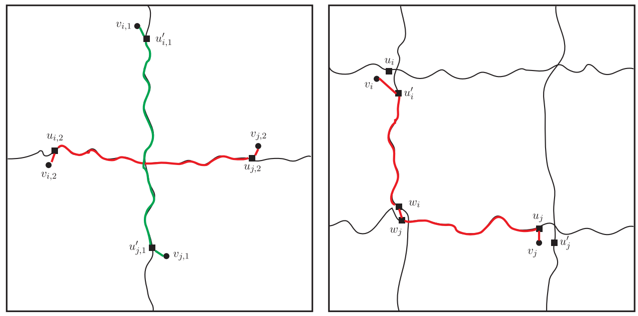

Fig. 2. Multicast path in a cluster-dense regime. Left: $u_{i,2}$ and $u_{j,2}$ are in the same horizontal crossing path and connected by the red sub-path $\mathcal{P}(\overline{u_{i,2}u_{j,2}})$. Right: v_i and v_j are connected by two red sub-path $\mathcal{P}(\overline{u_i' w_i})$ and $\mathcal{P}(\overline{w_j u_j})$.

(1) Case 1: the sender is not in the highway, the receiver is in the highway;
(2) Case 2: both the sender and the receiver are in the highway;
(3) Case 3: the sender is in the highway, the receiver is not in the highway.

Lemma 5.1. *For cases 1 and 3, the rate of the single-hop transmission is* $\lambda_{1,3}(n) = \Omega(n^{(\alpha-\frac{1}{2})\gamma}(\log n)^{\gamma-2})$ w.h.p.*; for case 2, the rate of the single-hop transmission is* $\lambda_2(n) = \Omega(n^{(\alpha-\frac{1}{2})\gamma})$ w.h.p..

Proof. For both case 1 and case 3, the sender and receiver are within the same rectangle with size $\sqrt{2}cl \times \sqrt{2}c(\kappa \log l - \epsilon_l)$, and the horizontal distance between them is at most $\sqrt{2}c$. Thus, the Euclidean distance between them is at most $\sqrt{2}c(\kappa \log l + 1)$ ensured by triangle inequality.

Let $r = \sqrt{2}c(\kappa \log l + 1) = \Theta(c \log n)$ and $R = 2r$, and to achieve the data rate in Lemma 4.1, we partition the network region $\mathcal{B}$ into a number of small cells with side length r. According to the definition of cluster-dense regime, we have $\alpha < \nu/2 < \frac{1}{2}$. Thus,

$$r \sim c \log n \sim \frac{\log n}{\sqrt{\overline{\Phi}}} \sim \frac{\log n}{\sqrt{n^{1-2\alpha}}} \sim n^{\alpha-\frac{1}{2}} \log n \to 0,$$

as $n \to \infty$. Then we divide the phase into nine time slots such that within a time slot, any two cells that contain senders is at least three cells away. Thus, the distance between any two senders is at least $R = 2r$. Besides, the nodes in the same cells have to share the bandwidth, the number of which is at most $2r^2\overline{\Phi}$ from Lemma 4.2. Therefore, *w.h.p.*, the data rate achievable of the links of case 1 and case 3 is at least

$$\begin{aligned}\frac{1}{2r^2\overline{\Phi}} \log\left(1 + \frac{P \cdot \min\{1, r^{-\gamma}\}}{N_0 + c_1 P \cdot (R-r)^{-\gamma}}\right) &\sim \frac{1}{\log^2 n} \log\left(1 + \frac{P}{N_0 + c_1 P \cdot r^{-\gamma}}\right) \\ &\sim \frac{1}{\log^2 n} \frac{P}{N_0 + c_1 P \cdot r^{-\gamma}} \\ &\sim \frac{r^\gamma}{\log^2 n} = n^{(\alpha-\frac{1}{2})\gamma}(\log n)^{\gamma-2}.\end{aligned} \tag{5}$$

In the same way, for case 2 the distance between sender and receiver is at most $2\sqrt{2}c$. Let $r = 2\sqrt{2}c$ and $R = 4\sqrt{2}c$, the rate achievable is $\Omega(n^{(\alpha-\frac{1}{2})\gamma})$. □

Since multiple flows for different multicast sessions may occupy the same link between two nodes, we need to take into account the number of multicast sessions per link.

LEMMA 5.2. *If node v is not in the highway, then* w.h.p. *it is contained in* $O(\frac{n_s k}{n})$ *multicast trees when* $n_s k = \omega(n)$*; if node v is in the highway, then* w.h.p. *it is contained in* $O(\frac{n_s\sqrt{k}}{\sqrt{n}})$ *multicast trees when* $k = O(\frac{n}{\log^2 n})$ *and* $n_s = \Omega(\frac{\sqrt{n}}{\sqrt{k}}\log n \log\frac{n}{k})$.

PROOF. The multicast tree $\mathrm{MT}(\mathcal{M})$ for each multicast session $\mathcal{M}$ contains a set of nodes in which some of them are in the highway and others are not. For any node v, the probability that node v is contained in the multicast session $\mathcal{M}$ is $\Pr(v \in \mathcal{M}) = \frac{k}{n}$. Let $\mathbf{1}_i$ be the indicator random variable of event $v \in \mathcal{M}_i$, and then $\Pr(\mathbf{1}_i = 1) = k/n$ and $\mathsf{E}[\mathbf{1}_i] = k/n$ for $i = 1, \ldots, n_s$. Since the multicast sessions are independent from each other, $\mathbf{1}_i$s are independent random variables and then $\mathsf{E}[\sum_{i=1}^{n_s}\mathbf{1}_i] = \sum_{i=1}^{n_s}\mathsf{E}[\mathbf{1}_i] = n_s k/n$. Using a Chernoff bound, we have

$$\Pr\left(\sum_{i=1}^{n_s}\mathbf{1}_i \geq (1+\delta)\frac{n_s k}{n}\right) \leq e^{-\frac{\delta^2}{2+\delta}\frac{n_s k}{n}}, \quad \forall\delta > 0.$$

If $\lim_{n\to\infty}\frac{n_s k}{n} = +\infty$, then *w.h.p.* $\sum_{i=1}^{n_s}\mathbf{1}_i = O(\frac{n_s k}{n})$. That is, if node v is not in the highway, then *w.h.p.* it is contained in $O(\frac{n_s k}{n})$ multicast trees.

Consider the construction of the multicast tree $\mathrm{MT}(\mathcal{M})$ in Algorithm 2, in which each edge of $\mathrm{EST}(\mathcal{M})$ is replaced by a horizontal and vertical edge. The Pythagorean theorem ensures that $|\mathrm{MT}(\mathcal{M})| \leq \sqrt{2}|\mathrm{EST}(\mathcal{M})|$, i.e., $|\mathrm{MT}(\mathcal{M})| = O(\sqrt{k}L)$. From Lemma 4.8 we have

$$|\mathrm{MT}(\mathcal{M})| \geq |\mathrm{EMST}(\mathcal{M})| = c(2)\sqrt{k}\int_{\mathcal{B}}\sqrt{\frac{\Phi(\xi)}{n}}d\xi = \Theta(\sqrt{k}L),$$

i.e., $|\mathrm{MT}(\mathcal{M})| = \Omega(\sqrt{k}L)$. Thus $|\mathrm{MT}(\mathcal{M})| = \Theta(\sqrt{k}L)$. Notice that the distance between the sender and receiver is $\Theta(c\log n)$ for case 1 and 3, $\Theta(c)$ for case 2. Let $N(\mathcal{M})$ be the number of nodes contained in multicast tree $\mathrm{MT}(\mathcal{M})$ that are in the highway, and then

$$|\mathrm{MT}(\mathcal{M})| - ck\log n \leq c\cdot(N(\mathcal{M})-1) \leq |\mathrm{MT}(\mathcal{M})|,$$

which implies $N(\mathcal{M}) = \Theta(\sqrt{k}\sqrt{n})$ when $k = O(n/\log^2 n)$. Hence, the probability that node v is in highway and is contained in multicast tree $\mathrm{MT}(\mathcal{M})$ is $\Theta(\sqrt{k}/\sqrt{n})$. Using VC-theorem, we have

$$\Pr\left(\sup_{v^*}\left|\frac{\#\text{ of multicast trees covering } v}{n_s} - \frac{\sqrt{k}}{\sqrt{n}}\right| < \epsilon(n)\right) > 1-\sigma(n)$$

if $n_s \geq \max\{\frac{8\log k}{\epsilon(n)}\cdot\log\frac{13}{\epsilon(n)}, \frac{4}{\epsilon(n)}\log\frac{2}{\sigma(n)}\}$. Let $\epsilon(n) = \sqrt{k}/\sqrt{n}$ and $\sigma(n) = 2/n$, and then we have

$$\Pr\left(\#\text{ of multicast trees covering } v \text{ is } O\left(n_s\sqrt{k}/\sqrt{n}\right)\right) > 1-2/n$$

if $n_s = \Omega(\frac{\sqrt{n}}{\sqrt{k}}\log n\log\frac{n}{k})$. □

For links in case 1 and case 3, the per-session data rate achievable is $\lambda_{1,3}(n)/O(\frac{n_s k}{n})$ when $n_s k = \omega(n)$; for links in case 2, the per-session data rate achievable is $\lambda_2(n)/O(\frac{n_s\sqrt{k}}{\sqrt{n}})$ when $k = O(n/\log^2 n)$ and $n_s = \Omega(\frac{\sqrt{n}}{\sqrt{k}}\log n\log\frac{n}{k})$. The per-session multicast capacity is the minimum achievable per-session data rate of single-hop links, i.e., $\lambda_2(n)/O(\frac{n_s\sqrt{k}}{\sqrt{n}})$, since it is smaller than $\lambda_{1,3}(n)/O(\frac{n_s k}{n})$. We summarize the performance of the routing and scheduling scheme for cluster-dense regime as follows.

Theorem 5.3. W.h.p. *the per-session multicast capacity for the cluster-dense regime is*

$$\lambda^{min}(n) = \Omega\left(n^{\frac{1}{2}+(\alpha-\frac{1}{2})\gamma}/n_s\sqrt{k}\right)$$

when $k = O(n/\log^2 n)$ *and* $n_s = \Omega(\frac{\sqrt{n}}{\sqrt{k}}\log n \log\frac{n}{k})$.

6 CLUSTER-SPARSE REGIME

In this section, we consider the cluster-sparse regime where $\lim_{n\to\infty} d_c = \infty$ and $\underline{\Phi} = \Theta(qs(d_c))$, $\overline{\Phi} = \Theta(q)$. This regime is more intricate than cluster-dense regime in two ways: (1) The local intensity $\Phi(\xi) = \Theta(qs(\min_j |\xi - c_j|))$ is more sophisticated than in cluster-dense regime, and (2) the approach used in cluster-dense regime is not applicable, since the number of nodes sharing the same entry point in highway blows up when n grows. We propose a multicast tree built upon nested highway systems to tame this difficulty.

6.1 Overview of the Scheme

Our approach is still based on the idea of extracting a subset $\mathbf{U}$ of nodes distributed according to an HPP of a given intensity, forming the infrastructure carrying data across the network. Since the variations of local intensity is larger than *cluster-dense* regime, it is impractical to extract only one subset of nodes $\mathbf{U}$ with intensity $\underline{\Phi}$ over the network to transfer data. Thus, we specify a nested highway systems $\{\mathcal{H}_h\}$ with a given sequence of intensities to facilitate the spread of information. We assume that $\underline{\Phi} = \Theta(n^\epsilon)$ for some $\epsilon > 0$. If this assumption does not hold, then we would select a head node for each cluster. These head nodes form a backbone that can be used to relay the data among different clusters.

6.2 Building Multicast Tree Using Nested Highways

We build a sequence of nested domains $\mathcal{B}_h$ (for $0 \le h \le H = \lfloor \log_2(\overline{\Phi}/\underline{\Phi})\rfloor$) defined as

$$\mathcal{B}_h = \left\{\xi \in \mathcal{B} : \Phi(\xi) \ge 2^h\underline{\Phi} = \zeta_h\right\}, \tag{6}$$

i.e., $\mathcal{B}_h$ is the region in which the local intensity exceeds threshold ζ_h. Let $\Delta\mathcal{B}_h$ be the region $\mathcal{B}_h - \mathcal{B}_{h+1}$ for $h = 0, 1, \ldots, H-1$ and $\Delta\mathcal{B}_H$ be the region $\mathcal{B}_H$, then $\{\Delta\mathcal{B}_h\}_{h=0}^H$ form a partition of the whole region $\mathcal{B}$. The local intensity of $\Delta\mathcal{B}_h$ is between ζ_h and $2\zeta_h$, i.e., $\zeta_h \le \Phi(\xi) \le 2\zeta_h$ for any $\xi \in \Delta\mathcal{B}_h$. Let $\partial\mathcal{B}_h$ be the boundary between region $\Delta\mathcal{B}_h$ and region $\Delta\mathcal{B}_{h+1}$ for $h = 0, \ldots, H-1$. Let $\mathbf{V}_h$ be all the nodes of $\mathbf{V}$ lying in $\mathcal{B}_h$.

Proposition 6.1 [3]. *For each h, a set of nodes* $\mathbf{U}_h \subset \mathbf{V}_h$ *can be found such that (1)* $\mathbf{U}_h$ *is a HPP of intensity* ζ_h *on* $\mathcal{B}_h$ *and (2) any node belonging to* $\mathbf{U}_{h-1}$ *and to* $\mathbf{V}_h$ *also belongs to* $\mathbf{U}_h$*, for* $h \ge 1$.

Using Proposition 6.1, we could build a nested highways $\{\mathcal{H}_h; h = 0, \ldots, H\}$. Similarly to the procedures in Section 5.2, for each h the highway $\mathcal{H}_h$ is built from the nodes $\mathbf{U}_h$ of intensity ζ_h and the cell length is $c_h = \Theta(1/\sqrt{\zeta_h})$. Then, Algorithm 3 is proposed to build a multicast tree $\mathcal{M}$ for each multicast session $\mathcal{M}$, in which $\mathcal{P}(\overline{u_1u_2})$ denotes the highway path between u_1 and u_2 if they are in the same highway.

As depicted in Figure 3, we use an example to show how Algorithm 3 works. Consider a multicast session $\mathcal{M} = \{v_1, v_2, \ldots, v_6\}$ and a network region consisted of five disjoint domains $\{\Delta\mathcal{B}_i\}_{i=0}^4$ satisfying Equation (6), i.e., the local intensity of $\Delta\mathcal{B}_i$ is between ζ_i and $2\zeta_i$. The nested highways $\{\mathcal{H}_i\}_{i=0}^4$ are constructed following the rules above. Suppose the nodes in $\mathcal{M}$ are not in the nested highways, and nodes $\{u_1, \ldots, u_6\}$ are the highway entry points for nodes in $\mathcal{M}$, respectively. We first build a Euclidean spanning tree EST($\mathcal{M}$). Then each edge of EST($\mathcal{M}$) is replaced by the nodes in the highways. Take the replacement of edge $\overline{v_1v_2}$ as an example. Observe that the edge $\overline{v_1v_2}$ crosses a sequence of boundaries $\partial\mathcal{B}_3, \partial\mathcal{B}_2, \partial\mathcal{B}_1, \partial\mathcal{B}_0$ from v_1 to v_2. We can find

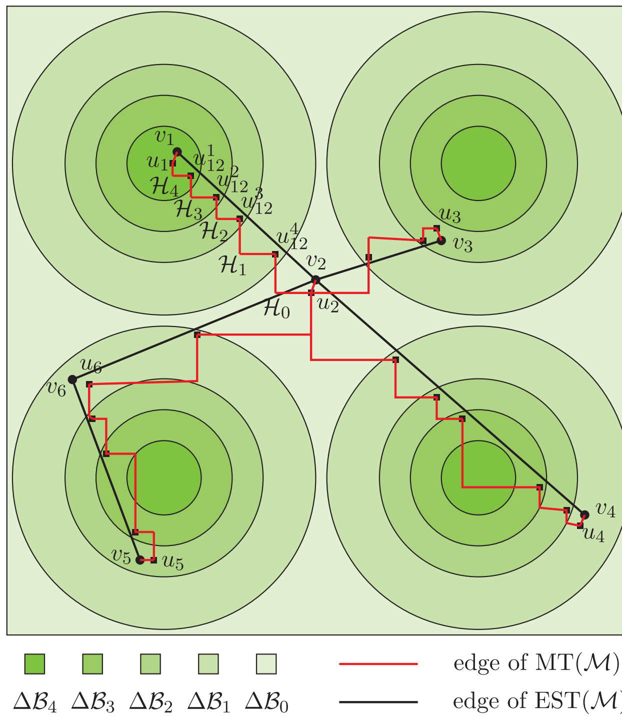

Fig. 3. Multicast tree in cluster-sparse regime.

ALGORITHM 3: Build Multicast Tree for Cluster-Sparse Regime

Input: A multicast session $\mathcal{M}$ consisted of k nodes.

MT′($\mathcal{M}$) ← $\mathcal{M}$;

Build a Euclidean multicast spanning tree EST($\mathcal{M}$) using Algorithm 1;

for *each edge* $\overline{v_i v_j}$ *in EST*($\mathcal{M}$) **do**

  Find the domain $\Delta\mathcal{B}_{h(v_i)}$ that v_i lies in and the corresponding highway entry point $u_i \in \mathcal{H}_{h(v_i)}$ for v_i;

  Find the domain $\Delta\mathcal{B}_{h(v_j)}$ that v_j lies in and the corresponding highway entry point $u_j \in \mathcal{H}_{h(v_j)}$ for v_j;

  $u_0 \leftarrow u_i$;

  Find the boundary sequence $\{\partial\mathcal{B}_h|\overline{v_i v_j}\}$ that the line $\overline{v_i v_j}$ crosses from v_i to v_j in $\mathcal{B}$;

  for *each boundary* $\partial\mathcal{B}_h$ *in* $\{\partial\mathcal{B}_h|\overline{v_i v_j}\}$ **do**

    Find a station node u_h in $\mathcal{H}_h \cap \mathcal{H}_{h+1}$(lying in $\mathcal{B}_{h+1}$) that is closest to the crossing point of $\partial\mathcal{B}_h$ and $\overline{v_i v_j}$;

    MT′($\mathcal{M}$) ← MT′($\mathcal{M}$) ∪ $\mathcal{P}(\overline{u_0 u_h})$; $u_0 \leftarrow u_h$;

  MT′($\mathcal{M}$) ← MT′($\mathcal{M}$) ∪ $\mathcal{P}(\overline{u_0 u_j}) \cup \overline{v_i u_i} \cup \overline{u_j v_j}$;

MT′($\mathcal{M}$) is a connected graph that covers $\mathcal{M}$. We could remove redundant edges and loops to get a multicast tree, denoted as MT($\mathcal{M}$);

Output: A multicast tree MT($\mathcal{M}$) using highway system.

---

four nodes $u_{12}^1, u_{12}^2, u_{12}^3, u_{12}^4$ from possibly different highways at the four crossing points. Then the nodes $\{u_1, u_{12}^1, u_{12}^2, u_{12}^3, u_{12}^4, u_2\}$ are connected using the nested highways and u_1 is connected to v_1 via one hop (so do u_2 and v_2). Repeat this procedure for all the edges in EST($\mathcal{M}$) and remove the redundant edges and loops; we will finally get the multicast tree MT($\mathcal{M}$).

6.3 Capacity Analysis

Though the multicast tree $\text{MT}(\mathcal{M})$ might contain nodes from possibly different highways, the single-hop transmission embedded in $\text{MT}(\mathcal{M})$ could still be classified into three cases based on whether the node is in the nested highways:

(1) Case 1: the sender is not in the nested highways, the receiver is in the nested highways;
(2) Case 2: both the sender and the receiver are in the nested highways;
(3) Case 3: the sender is in the nested highways, the receiver is not in the nested highways.

Lemma 6.2. *For cases 1 and 3, if the sender or receiver is in highway $\mathcal{H}_h$, then the rate of the single-hop transmission is $\lambda_{1,3}^h(n) = \Omega((\log n)^{\gamma-2}/\zeta_h^{\gamma/2})$* w.h.p. *for $h = 0, \ldots, H$; for case 2, if both the sender and receiver are in highway $\mathcal{H}_h$, then the rate of the single-hop transmission is $\lambda_2^h(n) = \Omega(\zeta_h^{-\gamma/2})$* w.h.p. *for $h = 0, \ldots, H$.*

Proof. For both case 1 and case 3, if the sender or receiver is in highway $\mathcal{H}_h$, then they are within the same rectangle with size $\sqrt{2}c_h l_h \times \sqrt{2}c_h(\kappa_h \log l_h - \epsilon_{l_h})$, where $l_h = L/c_h\sqrt{2}$, and the horizontal distance between them is at most $\sqrt{2}c_h$. The triangle inequality ensures that the distance between sender and receiver is at most $\sqrt{2}c_h(\kappa_h \log l_h + 1)$.

Let $r_h = \sqrt{2}c_h(\kappa_h \log l_h + 1) = \Theta(c_h \log n)$ and $R_h = 2r_h$. To achieve the data rate in Lemma 4.1, we partition the region $\Delta\mathcal{B}_h$ into a number of small cells with side length r_h. According to the definition of cluster-sparse regime, we have $\underline{\Phi} = \Theta(n^\epsilon)$ and thus

$$r_h \sim c_h \log n \sim \frac{\log n}{\sqrt{\zeta_h}} \to 0$$

as $n \to \infty$. Then we divide the phase into nine time slots such that within a time slot, any two cells that contain senders is at least three cells away. Thus, the distance between any two senders is at least $R_h = 2r_h$. Besides, the nodes in the same cells have to share the bandwith, the number of which is at most $4r_h^2\zeta_h$ from Lemma 4.2. Therefore, *w.h.p.*, the data rate achievable of the links of case 1 and case 3 is at least

$$\begin{aligned}\frac{1}{4r_h^2\zeta_h}\log\left(1+\frac{P\cdot\min\{1,r_h^{-\gamma}\}}{N_0+c_1P\cdot(R_h-r_h)^{-\gamma}}\right) &\sim \frac{1}{r_h^2\zeta_h}\log\left(1+\frac{P}{N_0+c_1P\cdot r_h^{-\gamma}}\right)\\ &\sim \frac{1}{r_h^2\zeta_h}\frac{P}{N_0+c_1P\cdot r_h^{-\gamma}}\\ &\sim \frac{r_h^{\gamma-2}}{\zeta_h} \sim \frac{(\log n)^{\gamma-2}}{\zeta_h^{\gamma/2}}.\end{aligned} \tag{7}$$

For case 3, if the sender and receiver are in highway $\mathcal{H}_h$, then the distance between them is at most $2\sqrt{2}c_h$. Let $r_h = 2\sqrt{2}c_h$ and $R_h = 4\sqrt{2}c_h$, and the rate achievable is $\Omega(\zeta_h^{-\gamma/2})$. □

Similarly to Lemma 5.2, we need to count the number of multicast sessions that occupy the same link. Different from the analysis in the cluster-dense regime, the sender and receiver of the link might belong to highway system $\mathcal{H}_h$ for any $h = 0, 1, \ldots, H$. We have the following results:

Lemma 6.3. *If node v is not in the nested highways, then* w.h.p. *it is contained in $O(\frac{n_s k}{n})$ multicast trees when $n_s k = \omega(n)$; if node v is in the highway $\mathcal{H}_h$, then* w.h.p. *it is contained in $O(\frac{n_s\sqrt{k}}{\sqrt{n}})$ multicast trees when $k = O(n/\log^2 n)$ and $n_s = \Omega(\frac{\sqrt{n}}{\sqrt{k}}\log n \log\frac{n}{k})$ for $h = 0, \ldots, H$.*

Proof. Consider the construction of the multicast tree $\mathrm{MT}(\mathcal{M})$ in Algorithm 3, in which each edge of $\mathrm{EST}(\mathcal{M})$ is replaced by a set of horizontal and vertical edges in different domains $\{\Delta\mathcal{B}_h\}$. Let $\mathrm{MT}(\Delta\mathcal{B}_h)$ be the set of edges of $\mathrm{MT}(\mathcal{M})$ lying in domain $\Delta\mathcal{B}_h$ for $h = 0, \ldots, H$. Let k_h be the number of nodes from $\mathcal{M}$ lying in domain $\Delta\mathcal{B}_h$, then *w.h.p.* $k\zeta_h|\Delta\mathcal{B}_h|/n \le k_h \le 2k\zeta_h|\Delta\mathcal{B}_h|/n$, i.e., $k_h = \Theta(k\zeta_h|\Delta\mathcal{B}_h|/n)$ and $\lim_{n\to\infty} k_h = \infty$. Using the Pythagorean theorem, we have $|\mathrm{MT}(\Delta\mathcal{B}_h)| \le \sqrt{2}|\mathrm{EST}(\Delta\mathcal{B}_h)|$, i.e., $|\mathrm{MT}(\Delta\mathcal{B}_h)| = O(\sqrt{k/n}|\Delta\mathcal{B}_h|\sqrt{\zeta_h})$. From Corollary 4.9, we have

$$|\mathrm{MT}(\Delta\mathcal{B}_h)| \ge |\mathrm{EMST}(\Delta\mathcal{B}_h)| = c(2)\sqrt{k_h}\sqrt{|\Delta\mathcal{B}_h|} = \Theta(\sqrt{k/n}|\Delta\mathcal{B}_h|\sqrt{\zeta_h}),$$

and, therefore, $|\mathrm{MT}(\Delta\mathcal{B}_h)| = \Theta(\sqrt{k/n}|\Delta\mathcal{B}_h|\sqrt{\zeta_h})$. Let $N(\Delta\mathcal{B}_h)$ be the number of nodes that are in the highway $\mathcal{H}_h$ and contained in multicast tree $\mathrm{MT}(\mathcal{M})$, then

$$|\mathrm{MT}(\Delta\mathcal{B}_h)| - c_h k_h \log n \le c_h \cdot (N(\Delta\mathcal{B}_h) - 1) \le |\mathrm{MT}(\Delta\mathcal{B}_h)|,$$

yielding $N(\Delta\mathcal{B}_h) = \Theta(\sqrt{k/n}|\Delta\mathcal{B}_h|\zeta_h)$ when $k = O(n/\log^2 n)$. Hence, the probability that node v is in nested highways and is contained in multicast tree $\mathrm{MT}(\mathcal{M})$ is

$$\frac{1}{n}\sum_{h=0}^{H} N(\Delta\mathcal{B}_h) \sim \frac{1}{n}\sum_{h=0}^{H}\sqrt{\frac{k}{n}}|\Delta\mathcal{B}_h|\zeta_h \sim \sqrt{\frac{k}{n}}.$$

Using VC-theorem, we have

$$\Pr\left(\#\text{ of multicast trees covering } v \text{ is } O(n_s\sqrt{k}/\sqrt{n})\right) > 1 - \frac{2}{n}$$

if $n_s = \Omega(\frac{\sqrt{n}}{\sqrt{k}}\log n \log\frac{n}{k})$. □

For links in case 1 and case 3, the per-session data rate achievable is $\lambda_{1,3}^h(n)/O(\frac{n_s k}{n})$ when $n_s k = \omega(n)$ for $h = 0, \ldots, H$; for links in case 2, the per-session data rate achievable is $\lambda_2^h(n)/O(\frac{n_s\sqrt{k}}{\sqrt{n}})$ when $k = O(n/\log^2 n)$ and $n_s = \Omega(\frac{\sqrt{n}}{\sqrt{k}}\log n\log\frac{n}{k})$ for $h = 0, \ldots, H$. The per-session multicast capacity is the minimum one among all the feasible rate for case 1, 2, 3 and for $h = 0, \ldots, H$, i.e., $\lambda_2^H(n)/O(\frac{n_s\sqrt{k}}{\sqrt{n}})$.

Theorem 6.4. W.h.p. *the per-session multicast capacity for the cluster-sparse regime is*

$$\lambda^{min}(n) = \Omega\left(n^{\frac{1}{2}-(1-\nu)\gamma/2}/n_s\sqrt{k}\right)$$

when $k = O(n/\log^2 n)$ *and* $n_s = \Omega(\frac{\sqrt{n}}{\sqrt{k}}\log n\log\frac{n}{k})$.

7 MULTICAST CAPACITY UPPER BOUND

To study the upper bound of per-session multicast capacity, we should get rid of the limitations of network operation strategy and only consider the restriction of physical limitations. Exploiting the relation between max-flow and min-cut, we first analyze the largest load of some cut for any routing and scheduling scheme and then use the capacity bottleneck imposed by the Gaussian channel model to obtain the asymptotic upper bound.

7.1 Largest Load for Some Cut

To study the load of a cut, we need to find some cuts in the heterogeneous network. We consider a rectangle of size $d_c/2 \times L$ located in between two adjacent columns of clusters centers, as illustrated by the shaded area in Figure 4. We observe that the local intensity is $\Phi(\xi) = \Theta(qs(d_c))$ at any point ξ within the considered rectangle. Thus the maximum intensity within the rectangle, denoted by Φ', is found at points located at distance $d_c/4$ from one cluster center.

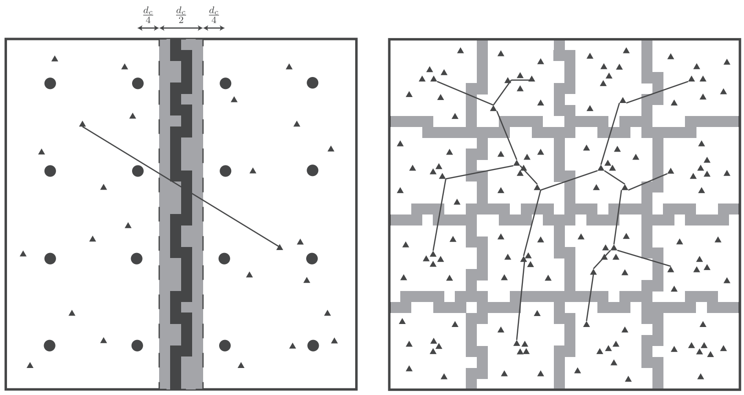

Fig. 4. Empty cut in the heterogeneous network.

We divide the above rectangle into small squarelets Z of area $|Z|$ and edge length z. The area $|Z|$ can be set in such a way that the probability p that an arbitrary squarelet within the rectangle contains no node is larger than the critical probability $p_c^s \approx 0.59$ of independent site percolation in the square lattice [16]. Having chosen $p > p_c^s$, the above condition is satisfied when $e^{-\Phi'|Z|} = p$, i.e., by setting $|Z| = -\log p/\Phi'$, then $z = \sqrt{|Z|} = \Theta(1/\sqrt{\Phi'}) = o(d_c/\log n)$. By this choice of $|Z|$, percolation results similar to those exploited in Reference [10] gaurantee *w.h.p.* the existence, within the considered rectangle, of at least one path (actually, $\Theta(d_c/z)$ non-overlapping paths) formed by empty squares and connecting the top edge with the bottom edge of the rectangle. An example of top-to-bottom crossing path is depicted in Figure 4. Such paths behave almost as straight lines, and in fact there exists *w.h.p.* at least one crossing path comprising $\Theta(L/z)$ squares of area $|Z|$. The largest load of this empty cut is presented in the following lemma.

Lemma 7.1. *For any empty cut composed of $\Theta(L/z)$ empty squares of side length z, the amount of information that can flow across it is $O((L/z)^\gamma)$.*

Proof. See Appendix C. □

7.2 Capacity Upper Bound

Theorem 7.2. *The per-session multicast capacity is*

$$\lambda^{min}(n) = O\left((L\sqrt{qs(d_c)})^\gamma / n_s\sqrt{k}\right).$$

Proof. We have shown in Lemma 7.1 that the amount of information that can flow across an empty cut is upper bounded by $O((L/z)^\gamma)$. To obtain an upper bound of the per-session multicast capacity, it suffices to derive a lower bound of the number of multicast sessions crossing the empty cut. Note that there exists at least one empty cut between two adjacent columns of cluster centers. Since each column/row contains $\sqrt{m}$ cluster centers, we could build $2\sqrt{m}$ empty cuts in total uniformly distributed over the whole network region $\mathcal{B}$. These cuts partition the whole network region into m super-cells with nearly equal size $\Theta(d_c^2)$. Since the number of super-cells crossed by any multicast tree $\mathrm{MT}(\mathcal{M})$ is at least $\lceil|\mathrm{EMST}(\mathcal{M})|/d_c\rceil = \Theta(\sqrt{k}L/d_c)$ and there are n_s independent multicast trees, we have *w.h.p.* $\Omega(n_s\sqrt{k}L/d_c)$ total load of all the m super-cells. Note that if a multicast tree crosses two super-cells, then it will cross at least one empty cut. Therefore, the total number of multicast flows crossing the empty cuts is $\Omega(n_s\sqrt{k}L/d_c)$. Since there are $2\sqrt{m}$ empty cuts, according to pigeonhole principle there is at least one empty cut that will be occupied by

$\Omega(\frac{n_s\sqrt{k}L}{d_c\sqrt{m}}) = \Omega(n_s\sqrt{k})$ sessions. Therefore, the per-session multicast capacity is upper bounded by

$$\frac{(L/z)^\gamma}{n_s\sqrt{k}} \sim \frac{(L\sqrt{qs(d_c)})^\gamma}{n_s\sqrt{k}}. \qquad \square$$

8 ASYMPTOTIC ENERGY EFFICIENCY

The energy $\mathcal{E}_\mathcal{S} = (E_1, \ldots, E_{n_s})$ consumed to achieve the per-session multicast capacity is determined by the data forwarding scheme and the allocated power for each node. We first compare the canonical uniform power allocation strategy to the dynamic power allocation strategy and then analyze the asymptotic per-session energy efficiency.

8.1 Asymptotic Optimal Power Allocation Strategy

The allowed emitted power ranges from $\underline{P}$ to $\overline{P}$ for each node. Define the uniform power allocation strategy $\mathcal{U}(P)$ as the strategy that each node sets its emitted power to the same value $P \in [\underline{P}, \overline{P}]$. We will show in the following lemma that this simple uniform power allocation scheme is asymptotically optimal.

Lemma 8.1 (Asymptotic Optimal Power Allocation Scheme). *The uniform power allocation scheme $\mathcal{U}(P)$ is asymptotically optimal to achieve the asymptotic per-session multicast capacity.*

Proof. To prove that $\mathcal{U}(P)$ is asymptotically optimal, we need to show that any power allocation scheme brings no gain to $\mathcal{U}(P)$ with respect to energy efficiency asymptotically.

Using the routing and scheduling scheme in Algorithm 2 and Algorithm 3, at any time for any sender-receiver pair (s_i, v_i) the following conditions are satisfied:

- C1: The Euclidean distance $|s_i - v_i| \leq r$;
- C2: For any other sender s_k, $k \neq i$, the Euclidean distance $|s_k - v_i| \geq R > r$.

Let V_S be the set of senders and V_R be the set of receivers. Suppose the power emitted by sender $s_i \in V_S$ is $P_i \in [\underline{P}, \overline{P}]$. For any receiver $v_i \in V_R$ and non-negative integer g, let

$$\mathcal{N}_g(v_i) = \{s \in V_S | g(R-r) \leq |v - s| < (g+1)(R-r)\}.$$

Let s_i be the intended sender of v_i, and $n_g(v_i) = |\mathcal{N}_g(v_i)|$ be the size of $\mathcal{N}_g(v_i)$. Constrained by C2, we have

$$n_g(v_i) \leq 2\left\lceil \frac{\pi(g+1)(R-r)}{(R-r)/2} \right\rceil = 2\lceil \pi(2g+2) \rceil.$$

Since $n_0(v_i) = 0$, the total interference at receiver v_i is

$$\begin{aligned} I(s_i, v_i) &\leq \sum_{g=1}^{\infty} \sum_{v \in \mathcal{N}_g(v_i)} P_v \cdot l(g(R-r)) \leq \sum_{g=1}^{\infty} n_g(v_i)\overline{P} \cdot l(g(R-r)) \\ &\leq \sum_{g=1}^{\infty} 2\lceil \pi(2g+2) \rceil \overline{P}(g(R-r))^{-\gamma} \leq \overline{P}(R-r)^{-\gamma} \sum_{g=1}^{\infty} 2\lceil \pi(2g+2) \rceil g^{-\gamma}. \end{aligned}$$

Since the sum $\sum_{g=1}^{\infty} 2\lceil \pi(2g+2) \rceil g^{-\gamma}$ converges when $\gamma > 2$, we have $I(s_i, v_i) \leq c_1\overline{P}(R-r)^{-\gamma}$, where c_1 is a constant depending on γ. Thus,

$$R(s_i, v_i) \geq \log\left(1 + \frac{\underline{P} \cdot l(r)}{N_0 + c_1\overline{P}(R-r)^{-\gamma}}\right),$$

yielding the same asymptotic results as $\mathcal{U}(P)$ when n approaches infinity. $\square$

8.2 Asymptotic Energy Efficiency

LEMMA 8.2. *For both cluster-dense and cluster-sparse regimes, the energy required to achieve the per-session multicast capacity lower bound is* $E(n) = \Theta(\sqrt{k}(\sqrt{k} + \sqrt{n}))$.

PROOF. For the cluster-dense regime, the multicast tree $\mathrm{MT}(\mathcal{M})$ contains about $k + N(\mathcal{M}) = \Theta(\sqrt{k}(\sqrt{k} + \sqrt{n}))$ nodes.

For the cluster-sparse regime, the number of nodes contained in $\mathrm{MT}(\mathcal{M})$ is about

$$k + \sum_{h=0}^{H} N(\Delta\mathcal{B}_h) = k + \sum_{h=0}^{H} \Theta(\sqrt{k/n}|\Delta\mathcal{B}_h|\zeta_h) = \Theta(\sqrt{k}(\sqrt{k} + \sqrt{n})).$$

If the asymptotic optimal power allocation scheme is used, then the required energy is $E(n) = \Theta(\sqrt{k}(\sqrt{k} + \sqrt{n}))$. □

THEOREM 8.3. *If* $k = O(n/\log^2 n)$ *and* $n_s = \Omega(\frac{\sqrt{n}}{\sqrt{k}} \log n \log \frac{n}{k})$, *for the cluster-dense regime, then the per-session energy efficiency is* $\eta(n) = \Omega(\frac{n^{\frac{1}{2}+(\alpha-\frac{1}{2})\gamma}}{n_s k(\sqrt{k}+\sqrt{n})})$; *for the cluster-sparse regime, the per-session energy efficiency is* $\eta(n) = \Omega(\frac{n^{\frac{1}{2}-(1-\nu)\gamma/2}}{n_s k(\sqrt{k}+\sqrt{n})})$. *And for both regimes* $\eta(n) = O((L\sqrt{qs(d_c)})^\gamma / n_s k(\sqrt{k} + \sqrt{n}))$.

9 EXPERIMENT AND SIMULATION

In this section, we empirically evaluate the performance of data forwarding schemes with respect to throughput and energy efficiency and compare it with the theoretic bounds. We discuss our experimental settings in Section 9.1 and present detailed empirical results in subsequent sections.

9.1 Simulation Setup

We evaluate our routing and scheduling schemes and theoretic bounds through simulations. We consider three synthetic networks with different heterogeneity, each with $N = 1000$ nodes, which are randomly deployed in a square $\mathcal{B}$ with side length $L = N^\alpha$, as shown in Figure 5(a)–(c). We estimate the density function Φ using Gaussian kernel and plot them using contours.

- For the *synthetic uniform benchmark*, the nodes are uniformly distributed over $\mathcal{B}$ with parameters $\alpha = 0.3$.
- For the *synthetic cluster-dense network*, the nodes are distributed based on model in Section 3.1 with parameters $\alpha = 0.3$, $\nu = 0.8$, and $\delta = 3.0$.
- For the *synthetic cluster-sparse network*, the nodes are distributed based on model in Section 3.1 with parameters $\alpha = 0.3$, $\nu = 0.4$, and $\delta = 3.0$.

Additionally, we take into account a real-world sensor network GreenOrbs [26], as shown in Figure 5(d). GreenOrbs is a large-scale operating sensor network system with up to 330 nodes deployed in the forest.

For each dataset, we designate n_s multicast sessions with size k. The number n_s takes values in $\{10, 20, \ldots, 100\}$, and the number k takes values in $\{10, 20, \ldots, 100\}$. Furthermore, for the channel model, we set the power attenuation factor $\gamma = 2.0$ and the Gaussian white noise $N_0 = 0.1$.

9.2 Evaluation of Throughput

First, we investigate the relation between achievable throughput and the number N of nodes. We construct a sequence of synthetic networks covering uniform benchmark, a cluster-dense regime, and a cluster-sparse regime for N in $\{500, 550, 600, \ldots, 1500\}$ and different α values and ν values. Then we compute the throughput with $k = 100$ and $n_s = 100$. The results are plotted in Figure 6.

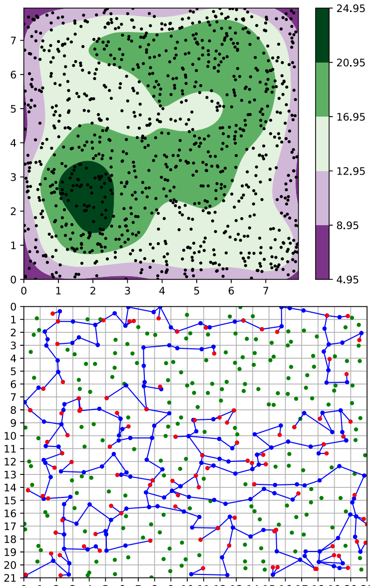

(a) uniform benchmark

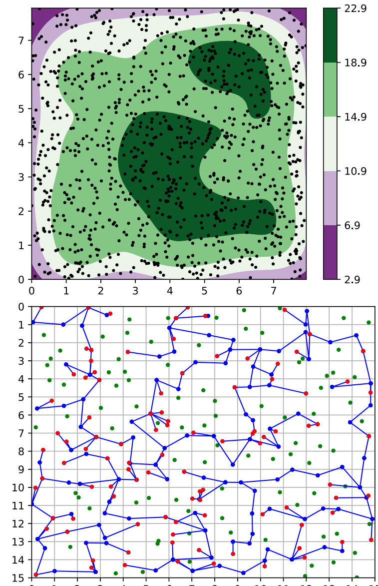

(b) cluster dense regime

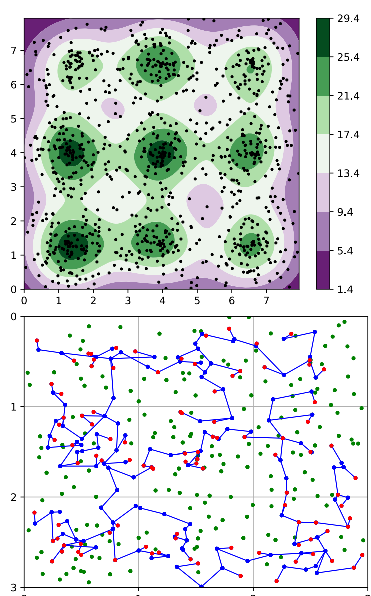

(c) cluster sparse regime

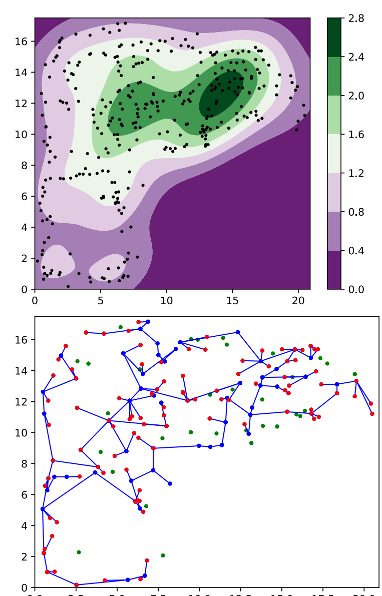

(d) greenorbs dataset

Fig. 5. Multicast routing for different types of networks. (1) The upper figures show the deployment of all the nodes by black dots and the estimated node density by contours. (2) The lower figures illustrate the multicast tree built for multicast sessions containing $k = 100$ nodes. The red dots represent 1 source node and 99 destination nodes. The green dots represent the stations contained in the highway systems. The blue dots represent the stations used as a relay in the routing.

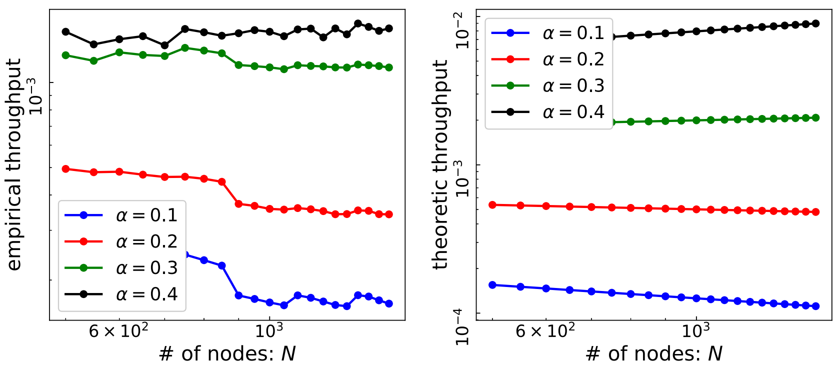

(a) uniform benchmark

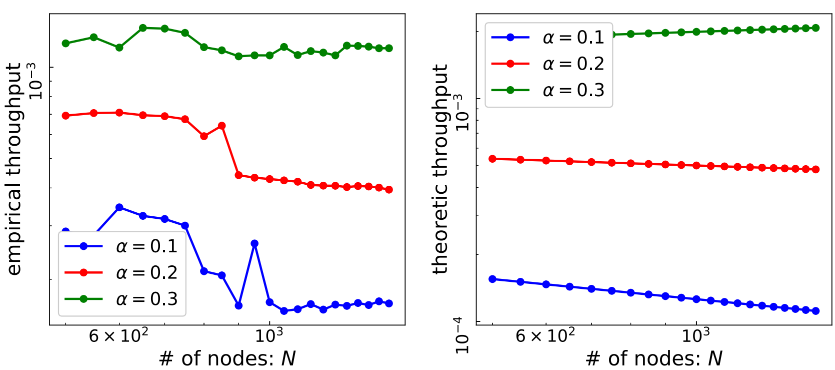

(b) cluster dense regime

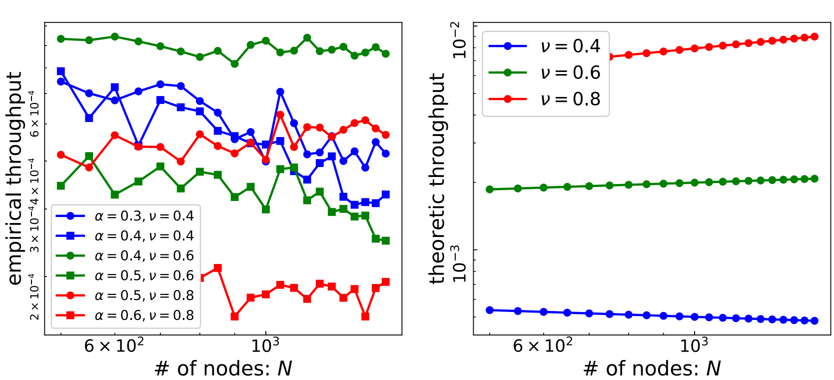

(c) cluster sparse regime

Fig. 6. The relation between throughput and the number of nodes.

As demonstrated in Figure 6(a) and (b), the throughput $\lambda^{\min}(n)$ approximates $n^{\frac{1}{2}+(\alpha-\frac{1}{2})\gamma}$ in proportion for the uniform benchmark and cluster-dense regime. Figure 6(c) tells that the throughput $\lambda^{\min}(n)$ approximates $n^{\frac{1}{2}-(1-\nu)\gamma/2}$ in proportion for the cluster-sparse regime.

Then we study the impact of multicast group size k on the achievable throughput. We designate a sequence of multicast groups over the four datasets and plot the results in Figure 7. Figure 7

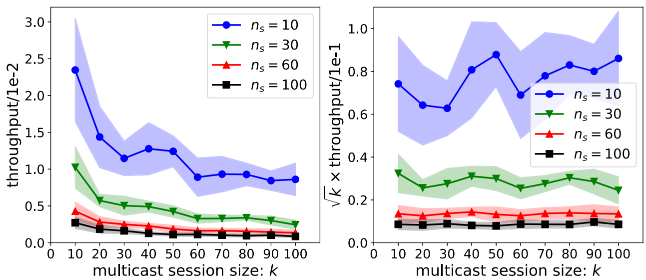

(a) uniform benchmark

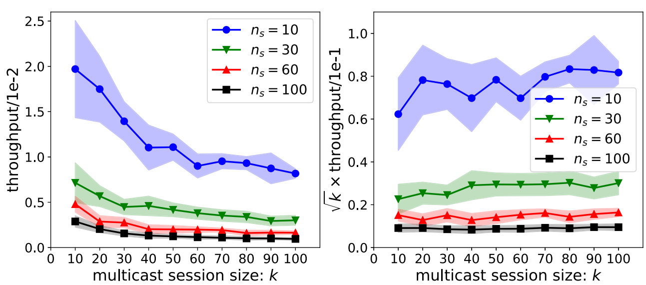

(b) cluster dense regime

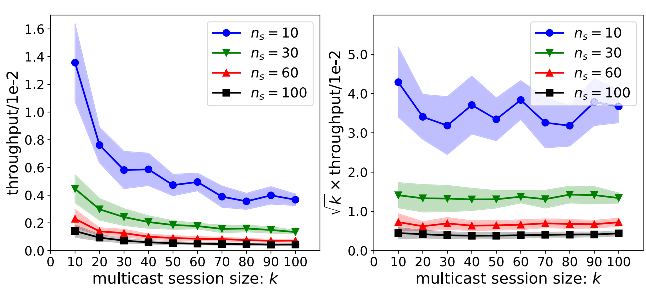

(c) cluster sparse regime

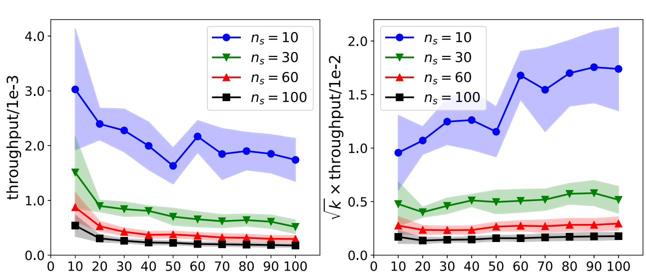

(d) greenorbs dataset

Fig. 7. Impact of multicast session size k on the throughput.

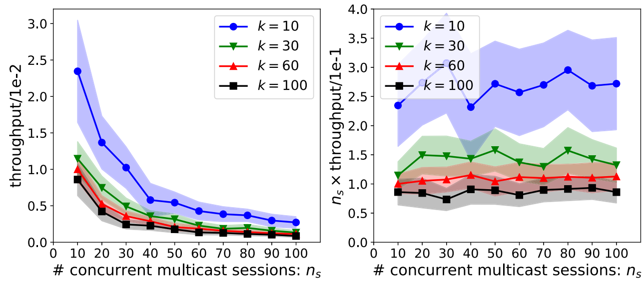

(a) uniform benchmark

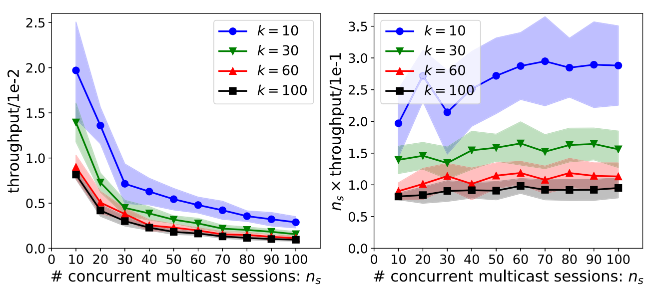

(b) cluster dense regime

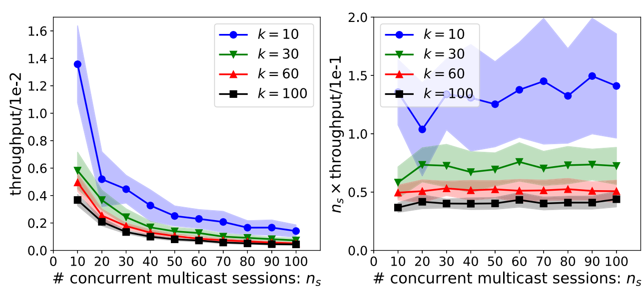

(c) cluster sparse regime

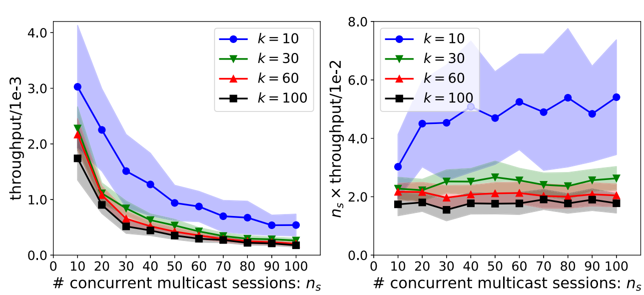

(d) greenorbs dataset

Fig. 8. Impact of the number n_s of concurrent multicast sessions on the throughput.

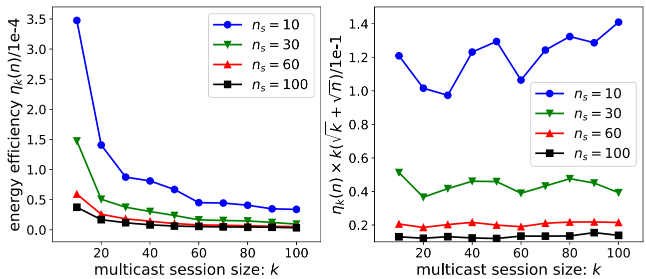

(a) uniform benchmark

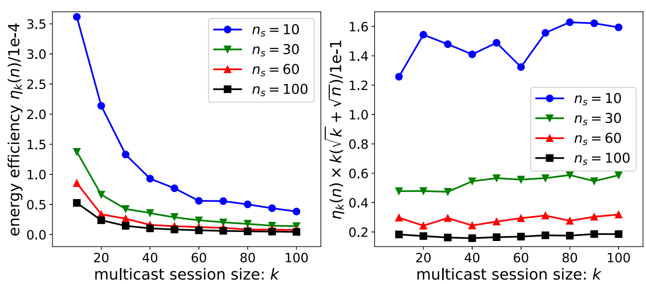

(b) cluster dense regime

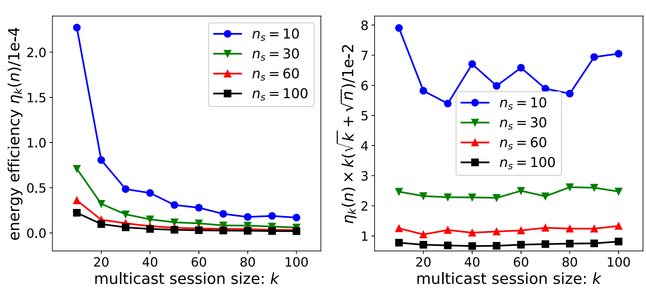

(c) cluster sparse regime

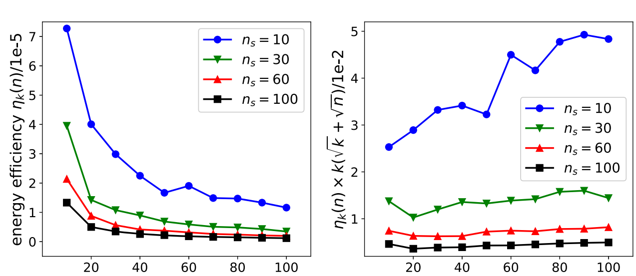

(d) greenorbs dataset

Fig. 9. Impact of multicast session size k on the energy efficiency $\eta_k(n)$.

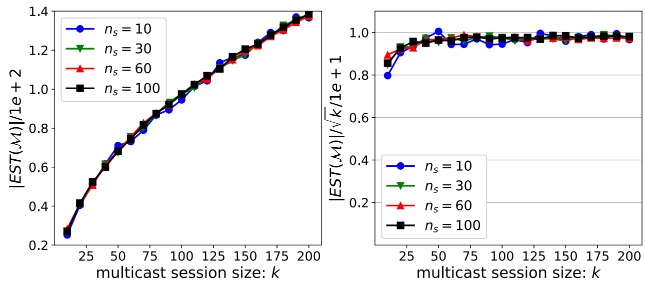

(a) uniform benchmark

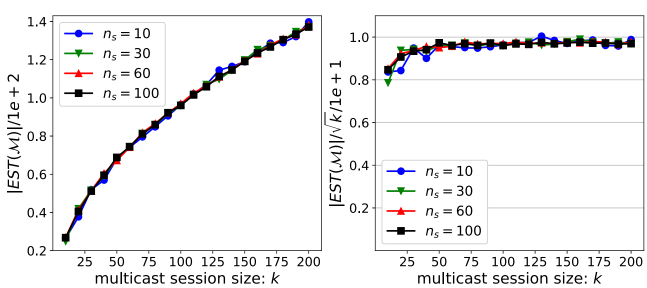

(b) cluster dense regime

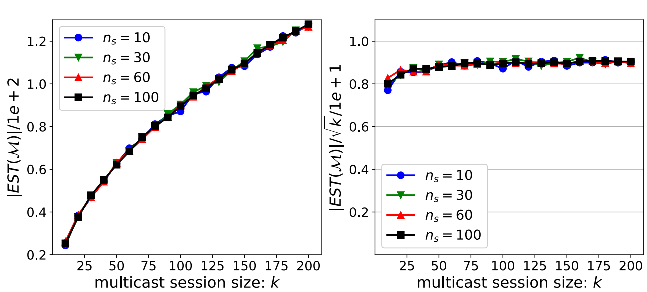

(c) cluster sparse regime

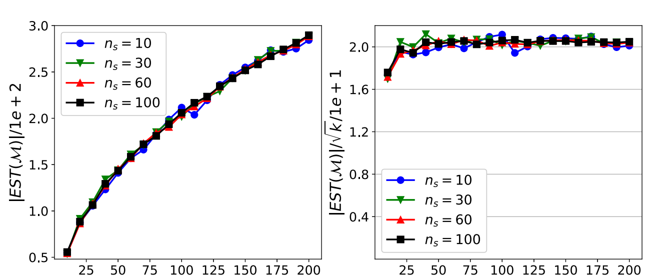

(d) greenorbs dataset

Fig. 10. The relation between multicast session size k and tree length $\mathrm{EST}(\mathcal{M})$.

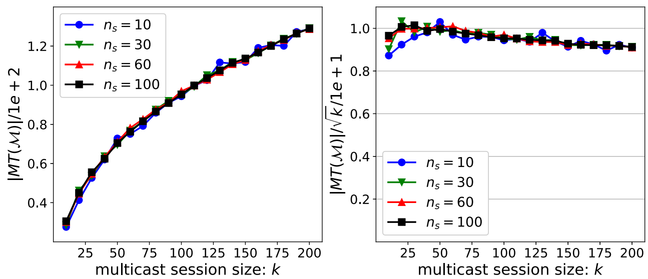

(a) uniform benchmark

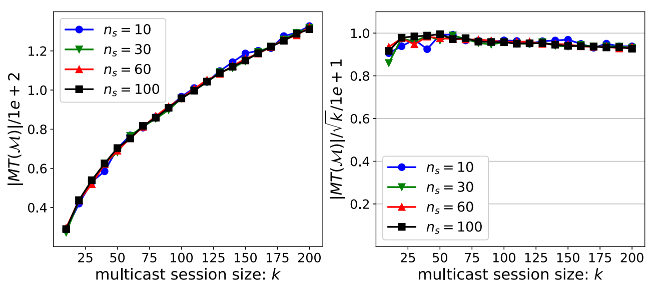

(b) cluster dense regime

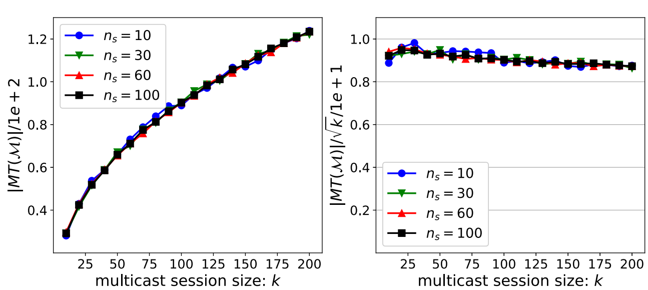

(c) cluster sparse regime

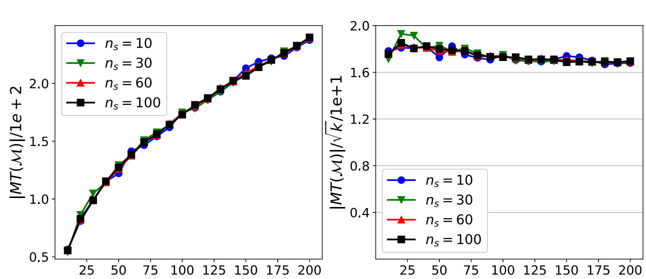

(d) greenorbs dataset

Fig. 11. The relation between multicast session size k and multicast tree length $|\mathrm{MT}(\mathcal{M})|$.

shows that the achievable throughput $\lambda^{\min}(n)$ is proportional to $1/\sqrt{k}$. Similarly, we study the impact of multicast group number n_s on the achievable throughput, and the results are plotted in Figure 8. Figure 8 tells that the achievable throughput $\lambda^{\min}(n)$ is proportional to $1/n_s$.

The results in Figures 6, 7, and 8 together validate the theoretic lower bound of throughput in Theorem 5.3 and Theorem 6.4.

9.3 Evaluation of Energy Efficiency

The energy efficiency $\eta(n)$ is highly related with the capacity $\lambda^{\min}(n)$ through the average number of hops for each multicast tree. We study the relation between $\eta(n)$ and $\sqrt{k}(\sqrt{k}+\sqrt{n})$, which is plotted in Figure 9. It tells that the achievable energy efficiency is proportional to $1/\sqrt{k}(\sqrt{k}+\sqrt{n})$. We omit the results of the rest of simulations, since they are similar to the evaluation of throughput.

9.4 Evaluation of Multicast Tree Length

Our empirical results also delineate the relation between tree length and tree size. As shown in Figure 10 and Figure 11, for any multicast group $\mathcal{M}$ with size $|\mathcal{M}| = k$, both the Euclidean spanning tree length $|\mathrm{EST}(\mathcal{M})|$ and the multicast tree length $|\mathrm{MT}(\mathcal{M})|$ are proportional to $\sqrt{k}$ in all four kinds of datasets.

10 CONCLUSION

In this article, we studied the multicast scaling laws of throughput and energy efficiency in heterogeneous wireless sensor networks. We first model the distribution of nodes' locations as a cluster process and then classify the networks into two regimes: a cluster-dense regime and a cluster-sparse regime. For different regime, we proposed a routing scheme based on multicast tree and percolation theory, aiming to provide throughput lower bound achievable solution. Combined with TDMA technique, we could achieve $\Omega(n^{\frac{1}{2}+(\alpha-\frac{1}{2})\gamma}/n_s\sqrt{k})$ throughput for the cluster-dense regime and $\Omega(n^{\frac{1}{2}-(1-\nu)\gamma/2}/n_s\sqrt{k})$ throughput for the cluster-sparse regime. Our experiments also reveal useful insights into the relation between n, n_s, k and the achievable throughput $\lambda^{\min}(n)$ and energy efficiency $\eta(n)$.

APPENDICES

A PROOF OF LEMMA 4.2

Before proving Lemma 4.2, we first give the Chernoff bound.

LEMMA A.1 (CHERNOFF BOUNDS). *Consider n i.i.d. random variables X_i taken values in $\{0,1\}$ with $p = \Pr(X_i = 1)$. Let $X = \sum_{i=1}^n X_i$, then $\mu = E(X) = np$ and*

- *Upper tail:* $\Pr(X \geq (1+\delta)\mu) \leq \exp(-\frac{\delta^2}{2+\delta}\mu), \forall\delta > 0;$
- *Lower tail:* $\Pr(X \leq (1-\delta)\mu) \leq \exp(-\frac{\delta^2}{2}\mu), \forall\delta \in (0,1).$

Suppose there are N nodes distributed over the network region uniformly at random. And $N/n^{2\alpha} = \Phi$ is satisfied when n is sufficiently large. Use $X_i \in \{0,1\}$ to denote the existence of ith node in the subsquare A_k. It follows that $\Pr(X_i = 1) = |A_k|/n^{2\alpha}$. Applying the Chernoff bound to the number of points of $\mathbf{U}$ falling in A_k, which is exactly $N(A_k) = \sum_{i=1}^N X_i$, we have

$$\Pr\left(N(A_k) \geq (1+\delta_1)\mu\right) \leq \exp\left(-\mu\delta_1^2/(2+\delta_1)\right), \forall\delta_1 > 0$$
$$\Pr\left(N(A_k) \leq (1-\delta_2)\mu\right) \leq \exp\left(-\delta_2^2\mu/2\right), \forall 0 < \delta_2 < 1,$$

where $\mu = \mathrm{E}(N(A_k)) = N|A_k|/n^{2\alpha} = \Phi|A_k|$. Let $\delta_1 = 1$ and $\delta_2 = 1/2$, we have $\Pr(N(A_k) \geq 2\Phi|A_k|) \leq e^{-\Phi|A_k|/3}$ and $\Pr(N(A_k) \leq \frac{\Phi|A_k|}{2}) \leq e^{-\Phi|A_k|/8}$. Hence,

$$\begin{aligned}\Pr\left(\Phi|A_k|/2 < N(A_k) < 2\Phi|A_k|\right) &= 1 - \Pr(N(A_k) \geq 2\Phi|A_k|) - \Pr(N(A_k) \leq \Phi|A_k|/2)\\ &\geq 1 - e^{-\Phi|A_k|/3} - e^{-\Phi|A_k|/8} = 1 - O\left(n^{-1}\right)\end{aligned}$$

if $|A_k| \geq 24\frac{\log n}{\Phi}$.

B PROOF OF THE ASYMPTOTIC LOCAL INTENSITY

Consider a generic point $\xi_0 \in \mathcal{B}_n$. By definition

$$\Phi(\xi_0) = \sum_{j=1}^{m} q \frac{s(|\xi_0 - c_j|)}{\int_{\mathcal{B}_n} s(|\zeta - c_j|)d\zeta} = \frac{q}{H}\sum_{j=1}^{m} s(|\xi_0 - c_j|),$$

where $H = \int_{\mathcal{B}_n} s(|\zeta - c_j|)d\zeta$ is a constant. To bound the intensity $\Phi(\xi_0)$, we need to evaluate the sum $\sum_{j=1}^{m} s(|\xi_0 - c_j|)$.

(1) When $d_c = \omega(1)$, function $s(\rho)$ simpifies to $\rho^{-\delta}$ where $\delta > 2$. We express the sum $\sum_{j=1}^{m} s(|\xi_0 - c_j|)$ by summing function $s(\rho)$ for all the cluster centers i vertical, horizontal, or diagonal steps away from ξ_0, for $i = 0, 1, \ldots, \frac{\sqrt{m}-1}{2}$. It follows that

$$\begin{aligned}\sum_{j=1}^{m} s(|\xi_0 - c_j|) &\geq s\left(\sqrt{2}d_c/2\right) + \sum_{i=1}^{\lfloor\frac{\sqrt{m}-1}{2}\rfloor} 8i \cdot s\left(\sqrt{2}(2i+1)d_c/2\right) = 2^{\frac{\delta}{2}} s(d_c)\left(1 + 8\sum_{i=1}^{\lfloor(\sqrt{m}-1)/2\rfloor} \frac{i}{(2i+1)^{\delta}}\right)\\ &\geq 2^{\frac{\delta}{2}} s(d_c)\left(1 + \frac{8}{3^{\delta}}\sum_{i=1}^{\lfloor(\sqrt{m}-1)/2\rfloor} i^{1-\delta}\right) \geq 2^{\frac{\delta}{2}} s(d_c)\left(1 + \frac{8}{3^{\delta}}\int_1^{\sqrt{m}/2} u^{1-\delta}du\right)\\ &= 2^{\frac{\delta}{2}}\left(1 + \frac{8}{3^{\delta}}\frac{1-(\sqrt{m}/2)^{2-\delta}}{\delta - 2}\right)s(d_c) = \Theta(s(d_c))\end{aligned}$$

$$\begin{aligned}\sum_{j=1}^{m} s(|\xi_0 - c_j|) &\leq s(1) + \sum_{i=1}^{\lceil(\sqrt{m}-1)/2\rceil} 8i \cdot s\left((2i-1)d_c/2\right) = s(1) + 8s\left(d_c/2\right)\sum_{i=1}^{\lceil(\sqrt{m}-1)/2\rceil} \frac{i}{(2i-1)^{\delta}}\\ &\leq s(1) + 8s\left(d_c/2\right)\left(1 + \sum_{i=2}^{\lceil(\sqrt{m}-1)/2\rceil} i^{1-\delta}\right) \leq s(1) + 2^{3-\delta}s(d_c)\left(1 + \int_1^{\infty} u^{1-\delta}du\right)\\ &= 1 + 2^{3-\delta}\left(1 + 1/(\delta-2)\right)d_c^{-\delta} = \Theta(1).\end{aligned}$$

Hence, if $d_c = \omega(1)$, then we have $\underline{\Phi} = \Theta(qs(d_c))$ and $\overline{\Phi} = \Theta(q)$. Actually, from the above two inequalities we could see that in order sense the dominant term in the sum $\sum_{j=1}^{m} s(|\xi_0 - c_j|)$ is the distance between closest cluster center to point ξ_0 under the mapping of $s(\cdot)$. So we can approximate the local intensity at point ξ_0 as $\Phi(\xi_0) = \Theta(qs(\min_{1\leq j\leq m}|\xi_0 - c_j|))$.

(2) When $d_c = O(1)$, we can approximate the sum $\sum_{j=1}^{m} s(|\xi_0 - c_j|)$ as follows as $n \to \infty$:

$$\sum_{j=1}^{m} s(|\xi_0 - c_j|) = \frac{1}{d_c^2}\sum_{j=1}^{m} s(|\xi_0 - c_j|)d_c^2 \approx \frac{1}{d_c^2}\sum_{j=1}^{m}\int_{C_j} s(|\xi_0 - \xi|)d\xi = \frac{1}{d_c^2}\int_{\mathcal{B}_n} s(|\xi_0 - \xi|)d\xi = \frac{H}{d_c^2}.$$

Consequently,

$$\Phi(\xi_0) = \frac{q}{d_c^2} = \frac{mq}{md_c^2} = \frac{n}{L^2}.$$

C PROOF OF LEMMA 7.1

We consider an arbitrary empty cut as illustrated in Figure 12. Our goal is to upper bound the amount of information $\mathcal{F}$ that can flow from right to left through the empty cut. We partition the right side of the empty cut into rectangles A_t, for $t = 1, 2, \ldots, \lfloor \log(L/z) - 1 \rfloor$, by drawing vertical lines at distance $2^{t-1}z$ from the empty cut, for $t = 1, 2, \ldots, \lfloor \log(L/z) - 1 \rfloor$. We want to evaluate the contribution $\mathcal{F}(A_t)$ of information sent by nodes in A_t through the cut.

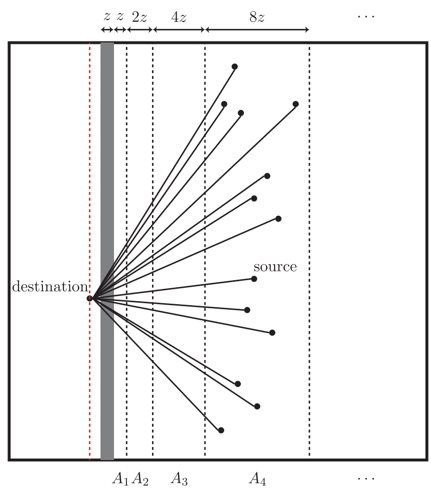

Fig. 12. Exponential tessellation of the right side of the empty cut.

Consider a generic rectangle A_t of edge $2^t z$ ($0 \le t \le \lfloor \log(L/z) - 1 \rfloor$). We have

$$\begin{aligned}
\mathcal{F}(A_t) &\le \sum_j \log\left(1 + \frac{P_j l(2^t z)}{N_0 + \sum_{i \ne j} P_i l(\sqrt{(2^t z)^2 + L^2})}\right) \\
&\le \sum_j \frac{P_j l(2^t z)}{N_0 + \sum_{i \ne j} P_i l(\sqrt{(2^t z)^2 + L^2})} \le \frac{l(2^t z)}{l(\sqrt{(2^t z)^2 + L^2})} \sum_j \frac{P_j}{\sum_{i \ne j} P_i} \\
&\le \frac{l(2^t z)}{l(\sqrt{(2^t z)^2 + L^2})} \sum_j \frac{2P_j}{\sum_i P_i} = 2\left(1 + \left(\frac{L}{2^t z}\right)^2\right)^{\gamma/2} \le 2^{1+\gamma/2} \left(\frac{L}{z}\right)^{\gamma} \left(\frac{1}{2^{\gamma}}\right)^{t}.
\end{aligned}$$

It follows that

$$\mathcal{F} \le \sum_{t=1}^{\lfloor \log(L/z) - 1 \rfloor} \mathcal{F}(A_t) \le 2^{1+\gamma/2} \left(\frac{L}{z}\right)^{\gamma} \sum_{t=1}^{\lfloor \log(L/z) - 1 \rfloor} \left(\frac{1}{2^{\gamma}}\right)^{t} \le 2^{1+\gamma/2} (L/z)^{\gamma} = \Theta((L/z)^{\gamma}).$$

REFERENCES

[1] I. F. Akyildiz, T. Melodia, and K. R. Chowdhury. 2007. A survey on wireless multimedia sensor networks. *Comput. Netw.* 51, 4 (2007), 921–960.

[2] Giusi Alfano, Michele Garetto, and Emilio Leonardi. 2009. Capacity scaling of wireless networks with inhomogeneous node density: Upper bounds. *IEEE J. Sel. A. Commun.* 27, 7 (Sept. 2009), 1147–1157.

[3] Giusi Alfano, Michele Garetto, Emilio Leonardi, and Valentina Martina. 2010. Capacity scaling of wireless networks with inhomogeneous node density: Lower bounds. *IEEE/ACM Trans. Netw.* 18, 5 (Oct. 2010), 1624–1636.

[4] Luigi Atzori, Antonio Iera, and Giacomo Morabito. 2010. The internet of things: A survey. *Comput. Netw.* 54, 15 (2010), 2787–2805.

[5] Adrian Baddeley. 2007. *Spatial Point Processes and Their Applications.* Vol. 1892. Springer, 1–75.

[6] Mario Di Francesco, Sajal K. Das, and Giuseppe Anastasi. 2011. Data collection in wireless sensor networks with mobile elements: A survey. *ACM Trans. Sens. Netw.* 8, 1, Article 7 (Aug. 2011), 31 pages.

[7] D. Z. Du and F. K. Hwang. 1992. A proof of the Gilbert-Pollak conjecture on the Steiner ratio. *Algorithmica* 7, 1 (01 Jun 1992), 121–135.

[8] E. J. Duarte-Melo and M. Liu. 2002. Energy efficiency of many-to-one communications in wireless networks. In *Proceedings of the 45th Midwest Symposium on Circuits and Systems*, Vol. 1. I–615.

[9] Enrique J. Duarte-Melo and Mingyan Liu. 2003. Data-gathering wireless sensor networks: Organization and capacity. *Comput. Netw.* 43, 4 (2003), 519–537.

[10] Massimo Franceschetti, Olivier Dousse, David N. C. Tse, and Patrick Thiran. 2007. Closing the gap in the capacity of wireless networks via percolation theory. *IEEE Trans. Inf. Theor.* 53, 3 (Mar. 2007), 1009–1018.

[11] L. Fu, X. Fu, Z. Zhang, Z. Xu, X. Wu, X. Wang, and S. Lu. 2018. Joint optimization of multicast energy in delay-constrained mobile wireless networks. *IEEE/ACM Trans. Netw.* 26, 1 (Feb. 2018), 633–646.

[12] A. El Gamal, M. Mohseni, and S. Zahedi. 2006. Bounds on capacity and minimum energy-per-bit for AWGN relay channels. *IEEE Trans. Inf. Theory* 52, 4 (Apr. 2006), 1545–1561.

[13] S. Gao, H. Zhang, and S. Das. 2009. Efficient data collection in wireless sensor networks with path-constrained mobile sinks. In *Proceedings of the 2009 IEEE International Symposium on a World of Wireless, Mobile and Multimedia Networks Workshops.* 1–9.

[14] Michele Garetto, Paolo Giaccone, and Emilio Leonardi. 2009. Capacity scaling in ad hoc networks with heterogeneous mobile nodes: The subcritical regime. *IEEE/ACM Trans. Netw.* 17, 6 (Dec. 2009), 1888–1901.

[15] M. Garetto and E. Leonardi. 2010. Restricted mobility improves delay-throughput tradeoffs in mobile ad hoc networks. *IEEE Trans. Inf. Theory* 56, 10 (Oct. 2010), 5016–5029.

[16] Geoffrey R. Grimmett. 1999. *Percolation.* Springer-Verlag.

[17] P. Gupta and P. R. Kumar. 2000. The capacity of wireless networks. *IEEE Trans. Inf. Theory* 46, 2 (Mar. 2000), 388–404.

[18] Wendi Rabiner Heinzelman, Joanna Kulik, and Hari Balakrishnan. 1999. Adaptive protocols for information dissemination in wireless sensor networks. In *Proceedings of the Annual International Conference on Mobile Computing and Networking (MobiCom'99).* ACM, New York, NY, 174–185.

[19] A. Jain, S. R. Kulkarni, and S. Verdu. 2011. Energy efficiency of decode-and-forward for wideband wireless multicasting. *IEEE Trans. Inf. Theory* 57, 12 (Dec. 2011), 7695–7713.

[20] A. Jain, S. R. Kulkarni, and S. Verdu. 2011. Multicasting in large wireless networks: Bounds on the minimum energy per bit. *IEEE Trans. Inf. Theory* 57, 1 (Jan. 2011), 14–32.

[21] S. R. Kulkarni and P. Viswanath. 2004. A deterministic approach to throughput scaling in wireless networks. *IEEE Trans. Inf. Theory* 50, 6 (2004), 1041–1049.

[22] Shi Li, Yunhao Liu, and Xiang-Yang Li. 2008. Capacity of large scale wireless networks under Gaussian channel model. In *Proceedings of the Annual International Conference on Mobile Computing and Networking (MobiCom'08).* ACM, New York, NY, 140–151.

[23] Xiang-Yang Li. 2009. Multicast capacity of wireless ad hoc networks. *IEEE/ACM Trans. Netw.* 17, 3 (Jun. 2009), 950–961.

[24] Xiang-Yang Li, Yunhao Liu, Shi Li, and ShaoJie Tang. 2010. Multicast capacity of wireless ad hoc networks under Gaussian channel model. *IEEE/ACM Trans. Netw.* 18, 4 (Aug. 2010), 1145–1157.

[25] Y. Li, Q. Peng, and X. Wang. 2014. Multicast capacity with max-min fairness for heterogeneous networks. *IEEE/ACM Trans. Netw.* 22, 2 (Apr. 2014), 622–635.

[26] Y. Liu, Y. He, M. Li, J. Wang, K. Liu, and X. Li. 2013. Does wireless sensor network scale? A measurement study on greenorbs. *IEEE Trans. Parallel Distrib. Syst.* 24, 10 (Oct. 2013), 1983–1993.

[27] M. Ma and Y. Yang. 2007. SenCar: An energy-efficient data gathering mechanism for large-scale multihop sensor networks. *IEEE Trans. Parallel Distrib. Syst.* 18, 10 (Oct. 2007), 1476–1488.

[28] M. Ma and Y. Yang. 2008. Data gathering in wireless sensor networks with mobile collectors. In *Proceedings of the 2008 IEEE International Symposium on Parallel and Distributed Processing.* 1–9.

[29] V. Rodoplu and T. H. Meng. 2007. Bits-per-Joule capacity of energy-limited wireless networks. *Trans. Wireless Comm.* 6, 3 (Mar. 2007), 857–865.

[30] Srinivas Shakkottai, Xin Liu, and R. Srikant. 2007. The multicast capacity of large multihop wireless networks. In *Proceedings of the International Symposium on Mobile Ad Hoc Networking and Computing (MobiHoc'07).* ACM, New York, NY, 247–255.

[31] L. Shangguan, Z. Yang, A. X. Liu, Z. Zhou, and Y. Liu. 2017. STPP: Spatial-temporal phase profiling-based method for relative RFID tag localization. *IEEE/ACM Trans. Netw.* 25, 1 (Feb. 2017), 596–609.

[32] J. Michael Steele. 1988. Growth rates of euclidean minimal spanning trees with power weighted edges. *Ann. Probab.* 16, 4 (10 1988), 1767–1787.

[33] S. Verdu. 1990. On channel capacity per unit cost. *IEEE Trans. Inf. Theory* 36, 5 (Sep. 1990), 1019–1030.

[34] Rolf H. Weber and Romana Weber. 2010. *Internet of Things: Legal Perspectives.* Springer-Verlag.

[35] J. E. Wieselthier, G. D. Nguyen, and A. Ephremides. 2000. On the construction of energy-efficient broadcast and multicast trees in wireless networks. In *Proceedings of the IEEE International Conference on Computer Communications (INFOCOM'00)*. 585–594.

[36] Feng Xia, Laurence T. Yang, Lizhe Wang, and Alexey Vinel. 2012. Internet of things. *Int. J. Commun. Syst.* 25, 9 (29 Aug. 2012), 1101–1102.

[37] Z. Zhang, M. Ma, and Y. Yang. 2008. Energy-efficient multihop polling in clusters of two-layered heterogeneous sensor networks. *IEEE Trans. Comput.* 57, 2 (Feb. 2008), 231–245.

Received September 2018; revised January 2019; accepted March 2019